Food and Bioprocess Technology (2020) 13:764–785
https://doi.org/10.1007/s11947-020-02407-y

ORIGINAL PAPER

Encapsulation of the Antioxidant Tyrosol and Characterization of Loaded Microparticles: an Integrative Approach on the Study of the Polymer-Carriers and Loading Contents

Filipa Paulo[1] · Lúcia Santos[1]

Received: 4 September 2019 / Accepted: 20 January 2020 / Published online: 25 March 2020

Abstract

Tyrosol, a powerful antioxidant present in high amounts in olive oil and mill wastes, possesses relevant health benefits due to its antioxidant properties. Therefore, tyrosol is a promising compound for further incorporation in functional foods. However, its incorporation in food matrices is limited due to its hydrophilicity. Therewith, encapsulation by double emulsion solvent evaporation emerges as an alternative for its protection and incorporation in lipophilic matrices, as some foods. This work aimed to encapsulate tyrosol in alternative carriers—poly(D,L-lactide-*co*-glycolide), ethylcellulose, and polycaprolactone, using two theoretical loading contents (TLC) (5% and 10% *w*/*w*). Tyrosol was efficiently incorporated in the selected polymer-carriers. Significant effects of the TLC were found on the product yield, encapsulation efficiency, thermal stability, morphology, and on the particle size distribution. This is the first study regarding the encapsulation of tyrosol and brings new insights concerning the encapsulation of antioxidants for further incorporation in food matrices.

Keywords Tyrosol · Encapsulation · Antioxidant · Loading · Polymer-carriers · Olive oil

Introduction

The worldwide recognition of the positive health effects of the Mediterranean diet has fostered the consumption of its typical foods. This dietary pattern is based on the consumption of olive oil as the primary source of fat; it also considers the high to moderate consumption of fruits, vegetables, and fish, and low consumption of wine and meat (Castro-quezada et al. 2014; Malheiro et al. 2012; Vlachogianni et al. 2015).

The positive health effects associated to this dietary pattern include the general reduction of the morbidity and the mortality rates, the prevention of cardiovascular diseases, and the lower incidence of diabetes type 2 (Castro-quezada et al. 2014; Gómez-gracia et al. 2018; Mitrou et al. 2015; Ruiz-gutie et al. 2017; Sofi et al., 2010, 2013). It may also have positive effects in the prevention and treatment of certain types of cancer and neurodegenerative diseases (Castro-quezada et al. 2014; Couto et al. 2011; Sofi et al. 2010, 2013).

The Mediterranean diet was considered Intangible Cultural Heritage of Humanity since December 4, 2013, by United Nations Educational, Scientific, and Cultural Organization (UNESCO) (2013).

It has been suggested by the scientific community that the positive health benefits of the Mediterranean Diet are strongly correlated to the presence of specific micro-constituents as phenolic compounds (Fernández-mar et al. 2012; Nadtochiy et al. 2011). In this dietary pattern, the majority of the phenolic compounds are found in olives, extra virgin olive oil, and red wine (Cicerale et al. 2012; Fernández-mar et al. 2012).

Highlights
1. Tyrosol (TYR) is a powerful antioxidant present in high quantitates in olive oil.
2. TYR incorporation in foods is limited due to its hydrophilic nature.
3. TYR was encapsulated by a double emulsion solvent evaporation approach.
4. TYR was encapsulated using alternative polymer-carriers and loading contents.
5. Significant effects of the loading were found on TYR physicochemical properties.

✉ Lúcia Santos
santos@fe.up.pt

[1] LEPABE – Laboratory for Process Engineering, Environment, Biotechnology and Energy, Faculty of Engineering, University of Porto, Rua Dr. Roberto Frias, 4200-465 Porto, Portugal

Moreover, during the processing of olive oil, many olive mill residues are produced. Among them, it is claimed that olive mill wastewaters (De Marco et al. 2007; El-Abbassi et al. 2012; Visioli et al. 1999), olive leaves (Benavente-García et al. 2000; El and Karakaya 2009; Pereira et al. 2007) and olive pomace (Aldini et al. 2006; Lesage-Meessen et al. 2001; Obied et al. 2007) present high content of the phenolic compounds that have strong radical scavenging capacity, responsible for many health benefits associated to the Mediterranean diet.

Noticeably, tyrosol, also known as 2-(4-hydroxyphenyl)ethanol or alternatively, 4-(2-hydroxyethyl)phenol, is one of the most simple phenols found in olive oil and olive mill wastes. It well documented its unique biological properties acting as an effective and powerful antioxidant (Giovannini et al. 1999; Lee et al. 2016). Recent studies pointed out the outstanding proinflammatory activity of tyrosol (Chang et al. 2019; Sato et al. 2016; Serra et al. 2017). Moreover, it described its potential antigenotoxic activity, and it also described its effectiveness in the prevention of the apoptosis of keratinocytes (Lee et al. 2016; Salucci et al. 2015). Additionally, it was demonstrated that it prevents endothelial dysfunction, and it may inhibit platelet-induced aggregation (Carluccio et al. 2003; Petroni et al. 1995). Furthermore, it is documented that tyrosol may ameliorate hyperglycemia in rats (Chandramohan et al. 2015; Lee et al. 2016).

Even though tyrosol presents outstanding properties, its employment is not widely reported in dietary supplements or as an additive, bioactive ingredient, or even as a stabilizer in foods, pharmaceutical formulations, cosmetics, and other industrial formulations or recipes, probably as a consequence of its hydrophilic chemical nature. Moreover, tyrosol solubilization or even incorporation in lipid matrices, as many foods, cosmetics, and pharmaceutical formulations, is still challenging.

Moreover, it is reported that tyrosol presents low bioavailability as a consequence of its low absorption and high metabolism in the human liver and small intestine (Vlachogianni et al. 2015).

Therefore, microencapsulation arises a potential strategy for the incorporation of tyrosol in polymer-based systems compatible with lipophilic matrices (e.g., the majority of foods). The incorporation of tyrosol in lipophilic carriers compatible with food matrices (food grade polymers) allows not only to protect tyrosol from oxidative food matrix environments but also allows its controlled/sustained release, thus allowing other vital molecules present in food matrices to be protected (Aguiar et al., 2016, 2017; Zhou et al. 2017). Moreover, the inclusion of tyrosol-loaded microparticles in food matrices may boost the bioavailability of tyrosol. Additionally, tyrosol is an antioxidant, and therefore, it is susceptible to auto-oxidation processes. In this context, microencapsulation may potentiate the protection of this powerful antioxidant from auto-oxidation processes.

Microencapsulation has been highly studied for the incorporation of water-soluble phenolic compounds (e.g., hydroxytyrosol) and even phenolic compounds that present low bioavailability as resveratrol (Paulo and Santos 2018b; Veiga and Cla 2011; Vlachogianni et al. 2015).

Regarding the case of the incorporation of water-soluble compounds in lipophilic matrices, the most commonly used microencapsulation approach is the water-in-oil-water (w_1/o/w_2) double emulsion solvent evaporation technique. Accordingly, the internal aqueous phase (w_1) that contains the water-soluble compound is emulsified in an organic phase (o) containing the polymer matrix that will coat the active ingredient. Afterward, the primary emulsion obtained (w_1/o) is then re-emulsified in an external aqueous phase (w_2). Then after, the evaporation of the solvent and the hardening of microparticles are promoted (Paulo and Santos 2018a, b, 2019).

Many biocompatible polymers can be used as lipophilic coating materials that can be from a natural source or can be semi-synthetic or even totally synthetized. Among them, poly(D,L-lactide-*co*-glycolide) (PLGA) is one of the most commonly used polymers worldwide. It is a Food and Drug Administration (FDA)- and European Medicine Agency (EMA)-approved family of copolymers of lactic acid and glycolic acid (Danhier et al. 2012). Moreover, it is classified as a group of biocompatible and biodegradable polymers that presents versatile and adjustable mechanical properties and displays a wide range of erosion times (Makadia and Siegel 2012).

Other alternative water-insoluble polymers that can be applied for coating purposes of water-soluble compounds are polycaprolactone (PCL) and ethylcellulose (EC). The synthetic polymer PCL is an aliphatic polyester that combines repeated units of hexanoate (Labet and Thielemans 2009). It is a biocompatible and a biodegradable polymer that presents remarkable permeability and compatibility for many bioactive compounds (Chen et al. 2000). As an alternative, EC is a semi-synthetic cellulose-derived polymer widely used for microencapsulation proposes. Even though it is not a biodegradable polymer, it is a biocompatible one, suitable for the coating and protection of bioactive ingredients. It is soluble in many organic solvents like ketones, alcohols, esters among others; however, as it holds some hydroxyl groups on its backbone structure, it can uptake water through hydrogen bond formation between the free hydroxyl groups in EC and water (Murtaza 2012; Paulo and Santos 2018a). The availability of EC to uptake water depends on the ethylation degree of the polymer. A low ethylation degree indicates that the polymer possesses more hydroxyl groups on its backbone structure, and therefore, it can uptake water more efficiently. Therefore, this polymer-carrier is not only suitable for the protection of bioactive compounds but also allows the permeation and release of bioactive compounds in aqueous systems.

This work aimed to incorporate tyrosol in alternative polymer-carriers as poly(D,L-lactide-*co*-glycolide), ethylcellulose, and

polycaprolactone by $w_1/o/w_2$ double emulsion solvent evaporation approach. A comprehensive assessment of the effect of the theoretical loading content (TLC) chosen (5% *w/w* or 10% *w/w*) on relevant physicochemical properties of tyrosol-loaded microparticles was performed. Specifically, the effect of the theoretical loading content on the production yield, the actual loading content, the encapsulation efficiency, the thermal and thermogravimetric stability, the outer morphology, and the particle size distribution was evaluated.

Additionally, a qualitative assessment of the efficient incorporation of tyrosol in the selected polymer-carriers was accomplished by Fourier Transform Infrared Spectroscopy (FTIR). Moreover, an evaluation of the total antioxidant capacity of tyrosol-loaded microparticles was carried out through the analysis of the Cu^{2+} chelating activity of tyrosol incorporated in microparticles.

In this work, an in-depth study of the physicochemical properties of tyrosol-loaded microparticles was carried out. Considering the possibility of the future incorporation of tyrosol-loaded microparticles as food additives in functional foods, a prior and relevant study of the physicochemical properties of tyrosol-loaded microparticles, which will affect the microparticle behavior in the fortified foods, is presented in this study.

Experimental Procedures

Materials

Chemicals

Tyrosol standard (Ref. 188255-5G, $C_8H_{10}O_2$, CAS 501-94-0), polyvinyl alcohol used as the surfactant of the double emulsion (Ref: P8136-250G, 87-90% hydrolyzed, an average molecular weight of 30,000–70,000, CAS 9002-89-5) were purchased from Sigma-Aldrich Chemical (St. Louis, MO, USA). Moreover, the polymers used for the encapsulation of tyrosol, ethylcellulose (Ref: 433837-250G, viscosity of 46 cP, ethylation degree of 48%, CAS 9004-57-3), poly(D,L-lactide-*co*-glycolide (Resomer® RG 504, Ref: 739944-5G, viscosity of 0.45–0.6 dL/g, CAS 26780-50-7, lactide/glycolide 50/50) and polycaprolactone (Ref. 440744-250G, presentation in pellets ~3 mm, CAS 24980-41-4) were also obtained from Sigma-Aldrich Chemical (St. Louis, MO, USA).

Dichloromethane (Ref. ACRO433991000, CH_2Cl_2, CAS 1665-00-5) used as a solvent was purchased from VWR International (Fontenay-sous-Bois, France). The eluents used in the high-performance liquid chromatography (HPLC) apparatus for the quantification of tyrosol, namely methanol (HiPerSolv CHROMANORM® Reagent Ph. Eur. Grade, HPLC grade, purity ≥ 99.8%, Ref: 20864.320, CH4O, CAS 67-56-1), acetonitrile (LiChrosolv® Reagent Ph. Eur. grade, Supelco®, supplier Merck, VWR Ref: 1.00030.2500, C_2NH_3, CAS 75-05-8), as well as the pH regulator, acetic acid standardized solution 0.1 N (supplier Alfa-Aesar, Ref: 35567.K7, C2H4O2, CAS 64-19-7), were obtained from VWR International (Fontenay-sous-Bois, France).

A total antioxidant capacity assay kit (Ref. MAK187) was purchased from Sigma-Aldrich Chemical (St. Louis, MO, USA).

The water used in this work was de-ionized and double-distilled using a Millipore™ water purification system (Massachusetts, USA) having 18.2 Ω electrical resistivity. Specifically, in the case of ultrapure water (Ref. 83645.32, H_2O, CAS 7732-18-5) used in the eluent composition of the detection and quantification of tyrosol in the high-performance liquid chromatography (HPLC) apparatus was purchased from VWR International (Fontenay-sous-Bois, France).

All the reagents were either of chromatographic or analytical grade and used as received.

Methods

Preparation of the Tyrosol-Loaded Microparticles

The encapsulation of tyrosol into alternative coating materials as poly(D,L-lactide-*co*-glycolide) (PLGA), ethylcellulose (EC), and polycaprolactone (PCL) was performed by $w_1/o/w_2$ water-in-oil-in-water double emulsion solvent evaporation microencapsulation technique as described by Paulo and Santos (2018a, b, 2019).

Regarding its hydrophilicity degree, tyrosol was dissolved in ultrapure water. A stock solution (concentration of 15 g/L) was prepared by rigorous weighing of the standard in analytical scale Mettler Toledo AG245 balance (Columbus, OH, USA). From this stock, the working solution was prepared by dilution of different standard solutions corresponding to different loading contents of tyrosol in the internal aqueous phase (w_1). For the volume measurements of the standard solutions, 10–100 μL, 100–1000 μL, and 500–5000 μL were used micropipettes (Eppendorf, Hamburg, Germany). A standard control solution in ultrapure water of 0.5 g/L was prepared weekly from the stock solution. All solutions were stored at 4 °C in amber glass vials during the study.

Distinct polymers, namely PLGA, EC, and PCL, were considered in the present study regarding their hydrophilic properties. The polymer PLGA present higher hydrophilicity, followed by EC, being PCL, the most hydrophobic polymer investigated in this study. The polymers were dissolved in dichloromethane at a polymer concentration of 10 g/L, constituting the organic phase (o). The obtained polymer solutions were sonicated for 5 min in an ultrasonic bath (P Selecta, Barcelona, Spain).

The external aqueous phase (w_2) was constituted by 100 g of polyvinyl alcohol (PVA) solution at a concentration of 1%

w/w. The external aqueous phase was previously prepared the day before the encapsulation experiment. For that, 1 g of PVA polymer was dissolved in 99 g of ultrapure water, under magnetic stirring (stirring plate from AREX Digital, VELP Scientifica, Monza, Italy) at around 120 °C. The process was performed until the total clearance of the polymer solution. The polymer solution was left equilibrate to room temperature overnight. The exact amount of ultrapure water lost during the dissolution of the polymer was added before the encapsulation process.

For each experiment, the volume of 1 mL of the internal aqueous phase (w_1) was admixed with 10 mL of the organic phase (o) forming the primary emulsion–water-in-oil (w_1/o) and vortexed during 3 min. The obtained emulsion was re-emulsified in the external aqueous phase (w_2) using a high-performance homogenizer at 5000 rpm (IKA T18 Digital ULTRA-TURRAX®, Staufen, Germany), for 5 min. The evaporation of the solvent and the hardening of microparticles were performed by continuously stirring the w_1/o/w_2 double emulsion in a stirring plate (AREX Digital, VELP Scientifica, Monza, Italy) at 700 rpm for 3 h in the fume hood at room temperature.

Tyrosol-loaded microparticles were recovered by filtration using a 0.2 μm quantitative paper filter and washed with 500 mL of distilled water to remove polyvinyl alcohol residues. The recovered microparticles were frozen for 24 h at − 4 °C and freeze-dried for 72 h in a benchtop freeze-dryer (SP Scientific, NY, USA).

Two theoretical loading contents (TLCs) of tyrosol (5% *w/w* and 10% *w/w*) were evaluated for each polymer-carrier. The theoretical loading content (%, *w/w*) was appraised as the ratio between the weight of tyrosol added, and the sum of the weight of polymer and tyrosol added. The TLC (%, *w/w*) values chosen for this study are widely found as typical values in the literature. Therefore, in this study, the effectiveness of the encapsulation of tyrosol was evaluated using three polymers, each at two different TLCs, as presented in Table 1. All the experiments were performed in triplicate in a total formulation runs of 18 experiments. Further considerations are presented in Table 1.

Table 1 Experimental conditions of the study

Entry	Polymer	TLC (% *w/w*)	Polymer conc. (g/L)	PVA conc. (% *w/w*)
1	PLGA	5	10	1
2		10		
3	EC	5	10	1
4		10		
5	PCL	5	10	1
6		10		

Conc. concentration, *EC* ethyl cellulose, *PCL* polycaprolactone, *PLGA* poly(D,L-lactide-*co*-glycolide), *PVA* polyvinyl alcohol, *TLC* theoretical loading content

Physicochemical Characterization of Tyrosol-Loaded Microparticles

Determination of the Tyrosol Loading Content, the Encapsulation Efficiency, and the Product Yield

The tyrosol-loaded microparticles production yield (TPY) and the tyrosol actual loading content (TALC) were examined.

The tyrosol-loaded microparticle production yield was assessed through Eq. (1) as described by Jansen-Alves et al. (2019) when they encapsulated propolis extract by a spray-drying technique using pea protein as a wall material.

$$TYP\ (\%) = \frac{W_M}{W_A} \times 100 = \frac{W_M}{W_I + W_P} \times 100 \quad (1)$$

where W_M is the weight of tyrosol-loaded microparticles recovered after the freeze-drying process, W_A is the weight of tyrosol initially added for the encapsulation (W_I) and the weight of the polymer used for the encapsulation (W_P).

The actual loading content of tyrosol-loaded microparticles was evaluated considering Eq. (2).

$$TALC\ (\%) = \frac{W_T}{W_M} \times 100 = \frac{W_I - W_O}{W_M} \times 100 = \frac{W_I - (W_S + W_L)}{W_M} \times 100 \quad (2)$$

where W_T is the weight of tyrosol in the microparticles. The weight of tyrosol in the microparticles (W_T) was evaluated considering the difference between the weight of tyrosol initially added (W_I) and the weight of tyrosol non-encapsulated (W_0).

The weight of tyrosol non-encapsulated (W_0) was computed considering the weight of tyrosol present in the supernatant of 3 mL of the w_1/o/w_2 double emulsion after 3 h of microparticles hardening (W_S), when a sample of the w_1/o/w_2 double emulsion was submitted to a low-intensity centrifugation process (4000 rpm corresponding to 2670 G, using a centrifuge Rotofix 32A, Hettich) for 15 min. The supernatant (W_S) was collected and stored at − 20 °C, prior to analysis. The pellet containing microparticles was reconstructed in ultrapure water—the dissolution solvent of tyrosol—and again centrifuged for 15 min (low-intensity centrifugation process; 4000 rpm corresponding to 2670 G, using a Rotofix 32A centrifuge). The supernatant after this second centrifugation (W_L) was collected and stored at − 20 °C prior to analysis. Instrumental analysis was performed using a Merck Hitachi Elite LaChrom (Tokyo, Japan) high-performance liquid chromatography (HPLC) equipped with a Hitachi L-7100 pump and L-7250 autosampler and coupled to a L-7450A diode array detector. The HPLC analysis was conducted by using a Purospher® STAR RP-18 end-capped LiChroCART® column (250 mm × 4.0 mm, 5.0 μm) (Merck KGaA), attached to a guard column (4.0 mm × 4.0 mm, 5.0 μm) of the same type. The elution was performed as described by Tasioula-Margari and Tsabolatidou (2015) at a flow

rate of 1 mL/min, using a mobile phase composed by a mixture of ultrapure water/acetic acid (0.1 N) (97.5/2.5 *v*/*v*) (A) and methanol/acetonitrile (50/50 *v*/*v*) (B). The following elution gradient was adapted from the protocol presented by Tasioula-Margari and Tsabolatidou (2015): 95% of A and 5% of B as initial conditions kept during 5 min, 70% of A and 30% of B during 15 min (from minute 5 to minute 20) and then again, for the last 5 min, the initial conditions were reestablished (95% of A and 5% of B from the minute 20 to 25). The detection of tyrosol was performed at 280 nm. The quantification of tyrosol was performed after the computation of the obtained areas in a calibration curve previously obtained using different concentrations of the commercial standard of tyrosol.

The quantitative assessment of tyrosol encapsulation efficiency (TEE) was performed using Eq. (3), as previously described by Paulo and Santos (2018b).

$$TEE(\%\mathrm{w/w}) = \frac{W_T}{W_I} \times 100 = \frac{W_I - W_O}{W_I} \times 100 \quad (3)$$

The chromatographic analyses required for the assessment of tyrosol loading content and encapsulation efficiency were performed based on three independent assays.

FTIR Analysis

The qualitative assessment of the encapsulation efficiency of tyrosol-loaded microparticles was evaluated by FTIR method.

Samples were evaluated using the attenuated total reflectance (ATR) mode, with an A225/Q PLATINUM ATR Diamond crystal with a single reflection accessory. The spectra were recorded from 4000 to 500 cm^{-1} with a resolution of 4 cm^{-1}.

The absence of specific functional groups of tyrosol on the FTIR-ATR spectra indicates the efficient incorporation of tyrosol in the selected polymer-carriers.

Specifically, bands associated with the benzene ring present in the chemical structure of tyrosol should be carefully considered, such as (i) two bands relative to the C=C stretch (in-ring) from 1600 to 1400 cm^{-1} and (ii) out of the plane bending C-H, from 900 to 675 cm^{-1}.

Moreover, the comparison of FTIR spectra of unloaded microparticles, polymers, and tyrosol allows supporting the conclusions previously taken by the study of FTIR spectra of tyrosol-loaded microparticles. Each FTIR result presented and discussed in this work is based on the mean of three independent spectra obtained.

DSC Analysis

The differential scanning calorimetry (DSC) technique was selected to evaluate the thermal behavior of tyrosol-loaded microparticles, pure tyrosol, and the coating materials used in the present study (PLGA, EC, and PCL) as described by Paulo and Santos (2018b).

The analyses were performed in triplicate using a NETZSCH DSC 214 Polyma calorimeter (NETZSCH DSC 214 Polyma, Selb, Germany) with a temperature range of 30 to 270 °C at a heating rate of 10 K min^{-1}, under a nitrogen atmosphere (flow rate of 40 mL min^{-1}).

TGA

The thermogravimetric analyses (TGA) were employed to assess the thermal stability of tyrosol-loaded microparticles, pure tyrosol, and the polymers used as carriers of tyrosol as described by Piletti et al. (2017) and Paulo and Santos (2018b). Slight modifications were employed to the procedure proposed by Piletti et al. (2017).

The analyses were performed in triplicate using a Netzsch STA449 F3 Jupiter thermogravimetric analyzer (Netzsch STA449 F3 Jupiter, Selb, Germany) with a temperature range of 30 to 810 °C at a heating rate of 10 K min^{-1} under inert atmosphere (N_2, a flow rate of 30 mL min^{-1}).

Evaluation of the Morphology

The external morphology of tyrosol-loaded microparticles was evaluated according to the procedure described by Paulo and Santos (2018a, b, 2019).

Accordingly, the main external morphological characteristics of tyrosol-loaded microparticles, as well as microparticles polydispersity, were assessed using a PHENOM XL scanning light microscope (Eindhoven, The Netherlands) at an accelerating voltage of 10 kV.

Freeze-dried microparticles were placed on an aluminum stub with a carbon double-sided adhesive tape. The samples were sputter-coated with gold for 20 s using a vacuum-sputtering coater (Leica, EM SCD 500, Wetzlar, Germany).

Evaluation of the Particle Size Distribution

The particle size distributions of tyrosol-loaded PLGA microparticles, tyrosol-loaded EC microparticles, and tyrosol-loaded PCL microparticles were evaluated using the laser granulometry technique. The particle size distribution and polydispersity were evaluated for each formulation in triplicate using a Coulter Counter-LS 230 Particle Size Analyzer (Miami, FL, USA) equipment. Average values were considered in data analysis.

The polydispersity of particle size distributions was analyzed considering the polydispersity index (PDI) as presented in Eq. (4) as previously reported by Paulo and Santos (2018a, b, 2019).

$$PDI = \frac{D_{v,90} - D_{v,10}}{D_{v,50}} \quad (4)$$

where the $D_{v,\ 90}$, $D_{v,\ 10}$, and $D_{v,\ 10}$ represent the maximum particle diameter below which 90% of the sample volume exists, the maximum particle diameter below which 10% of the sample volume exists, and the maximum particle diameter below which 50% of the sample volume exists, respectively.

Evaluation of the Total Antioxidant Capacity of Tyrosol-Loaded Microparticles

The antioxidant capacity of tyrosol-loaded PLGA microparticles, tyrosol-loaded EC microparticles, tyrosol-loaded PCL microparticles, and pure tyrosol were evaluated using the total non-enzymatic antioxidant capacity (TAC) kit (Ref. MAK187, Sigma-Aldrich Chemical, St. Louis, MO, USA).

Similarly to the quantitative determination of tyrosol encapsulation efficiency into different polymer matrices, two concentrations were taken into account for the computing and calculation of the total antioxidant capacity of tyrosol-loaded microparticles—the equivalent concentration (C_S) of tyrosol present in the supernatant (T_S) in Trolox equivalents (TE) of the $w_1/o/w_2$ double emulsion after 3 h of microparticles hardening, when the sample of the $w_1/o/w_2$ double emulsion was submitted to a low-intensity centrifugation process (4000 rpm corresponding to 2670 G, using a centrifuge Rotofix 32A, Hettich) for 15 min and the corresponding concentration of tyrosol in a second supernatant (C_P) in TE, after the reconstruction of the pellet from the previous sample (T_P) in ultrapure water and its submission to a second centrifugation process for 15 min (low-intensity centrifugation process; 4000 rpm corresponding to 2670 G, using a Rotofix 32A centrifuge).

In brief, 100 μL of each sample were transferred to a 96-well plate. Afterward, 100 μL of Cu^{2+} working solution were added to all sample wells. The content was mixed by pipetting and incubated for 90 min at room temperature. The plate was protected from light during the incubation. Afterward, the absorbance was read at 570 nm in a microplate reader (Synergy HT, Biotek, USA) as described by Paulo and Santos (2018b). The authors applied the same technical approach for the determination of the antioxidant activity of hydroxytyrosol-loaded EC microparticles using two different theoretical loadings (5% *w*/*w* and 10% *w*/*w*) by double emulsion solvent evaporation technique.

A standard Trolox calibration curve was obtained, adding 0, 4, 8, 12, 16, and 20 μL of the 1 mM of the Trolox standard solution into the 96-well plate. Ultrapure water was added to each well to bring to volume to 100 μL. The 0, 4, 8, 12, 16, and 20 nmol/well standards were generated. All the measurements were performed in triplicate.

The results were obtained in TE of the unknown sample well. Results are expressed in mM of TE in the case of the working solutions prepared considering a TLC of 5% *w*/*w* and 10% *w*/*w* and in mg of TE/g of dried dispersion in the case of loaded microparticles.

Statistical Analysis

Data analyses were performed using the MINITAB 18 software (Minitab Inc., State College, PA, USA). The analysis of variance (ANOVA) was used to determine significant differences ($P < 0.05$).

The quantification of tyrosol was performed using the EZChrom Elite Chromatography Data System – Agilent (California, USA). The quantification of the antioxidant activity of tyrosol and tyrosol-loaded microparticles was executed using the Omega multiplate reader software.

Results

Even though it is well described that tyrosol presents remarkable radical scavenging activity, its potential incorporation in food matrices is still limited. To circumvent that, it is proposed, in the present study, its incorporation in polymer-carriers compatible with food matrices. Tyrosol-loaded microparticles were obtained by $w_1/o/w_2$ double emulsion solvent evaporation technique using three alternative polymer-carriers (PLGA, EC, and PCL). Moreover, for each polymer-carrier, two different TLCs were studied (5% *w*/*w* and 10% *w*/*w*). Additionally, the encapsulation efficiency and the radical scavenging potential of tyrosol and tyrosol-loaded microparticles were also evaluated as these parameters are considered to be relevant when the incorporation of loaded microparticles in functional foods is contemplated.

Furthermore, unloaded microparticles were produced and characterized similarly to tyrosol-loaded microparticles. The physicochemical characterization of polymer-only (PO) microparticles allowed to appraise some of the obtained results as well as it favored the interpretation of results and assumptions related to physicochemical properties of tyrosol-loaded microparticles. In the "Qualitative Assessment of Tyrosol Encapsulation Efficiency by FTIR" section, during the qualitative analysis of tyrosol encapsulation by FTIR-ATR, the comparison of the FTIR spectra of loaded microparticles with PO microparticles allows the prove that tyrosol was efficiently incorporated in the selected polymeric system as the presence of functional groups at similar wavenumbers of PO microparticles allows to infer about the surface similarity of the loaded and unloaded microparticles.

Analytical Methods Validation

The validation of the analytical methods was performed considering two complementary quantifications: (i) the quantification of tyrosol and (ii) the quantification of the total antioxidant capacity of loaded microparticles.

The methods were validated regarding the correlation coefficient, the relative standard error of the slope, the concentration range, the limit of detection (LOD), and the limit of quantification (LOQ) (part of the data is presented in Table 2).

In the case of the HPLC method, tyrosol was detected in ultrapure water and in the case of UV-Vis spectrophotometer method, the total amount of antioxidant encapsulated was evaluated considering the amount of antioxidants present in the external aqueous phase (polyvinyl alcohol solution at a concentration level of 1% *w/w*) after the hardening of microparticles (w_2).

For each method, a mean calibration curve was drawn based on the three independent calibration curves obtained. In the case of the HPLC method, a linear range was observed in the range of 1.0 mg/L to 15.0 mg/L, and in the case of the UV-Vis spectrophotometer method, a linear range was observed in the range of 2.0 to 20.0 nmol TE/L.

The LOD and LOQ obtained values for both calibration curves were acceptably low, demonstrating the possibility of the application of the obtained regression equations for the quantification of tyrosol as a single compound (HPLC method) or as an antioxidant (UV-Vis method).

Determination of the Tyrosol Loading Content and the Product Yield

The actual loading content (% *w/w*) and the product yield (% *w/w*) by referenced to the TLC (% *w/w*) of the different powders obtained are presented in Fig. 1 (Fig. 1a—actual loading content (% *w/w*) versus theoretical loading content; Fig. 1b—product yield (% *w/w*) versus theoretical loading content).

Considering the TLC of 5% *w/w*, the mean actual loading content of tyrosol-loaded PLGA, EC and PCL microparticles were 4.9 ± 0.1% *w/w*, 4.9 ± 0.1% *w/w*, and 4.7 ± 0.1% *w/w*, respectively. The amount of tyrosol per gram of dried dispersion was 49 ± 1 mg of tyrosol/g of dried dispersion, 49 ± 1 mg of tyrosol/g of dried dispersion, 49 ± 2 mg of tyrosol/g of dried dispersion, in the case of tyrosol-loaded PLGA, EC, and PCL microparticles, respectively.

The results of the actual loading content, considering a TLC of 10% *w/w* of tyrosol-loaded microparticles formulated using PLGA, EC, and PCL as polymer-carriers were 9.9 ± 0.1% *w/w*, 9.9 ± 0.1% *w/w*, and 9.5 ± 0.4% *w/w*, respectively. The amount of tyrosol per gram of dried dispersion was 99 ± 1 mg of tyrosol/g of dried dispersion using PLGA as the polymer-carrier, 99 ± 1 mg of tyrosol/g of dried dispersion in the case of using EC as the coating material and 95 ± 4 mg of tyrosol/g of dried dispersion, in the case of tyrosol-loaded PCL microparticles.

Regarding the statistical analysis, the actual loading content (% *w/w*) of tyrosol-loaded microparticles seemed not to be affected by the polymer chosen as the carrier for the encapsulation of tyrosol, as there were no observed statistically significant differences between the experimental groups (grouped by the polymer type) since the *P*-values obtained were 0.58 and 0.15 for a tyrosol load of 5% *w/w* and 10% *w/w*, respectively (considering a significance level of 95%). Not surprisingly, when the results are grouped by the TLC (5% *w/w* and 10% *w/w*), for each polymer was observed that actual loading content was dependent on the TLC ($P = 1.48 \times 10^{-8}$ in the case of using PLGA, 2.73×10^{-8} in the case of tyrosol-loaded EC microparticles and 4.08×10^{-5} when PCL was used as a coating material; for all cases, $P < 0.05$).

The results regarding the actual loading content support the efficient incorporation of tyrosol in different polymer-carriers. Moreover, microparticles can be tailored-made with alternative loadings, being the actual loading content of microparticles similar to the designed loading (the TLC). A similar trend was also observed by Yekdane and Goli (2019). The authors performed the encapsulation of pomegranate seed oil into alternative polymer-carriers (Arabic gum and xanthan gum). Accordingly, to the obtained results of the present study, the actual loading contents of pomegranate seed oil (ranged between 13.7 and 13.9%) were found to be similar to the

Table 2 Results from the regression analysis for the quantification of tyrosol and the total amount of antioxidants encapsulated

Analytical method validation parameters	HPLC method	UV-Vis method
Regression equation[a,b]	$A = (2.4 \pm 0.2) \times 10^5\ C\ (mg/L) + (-1.9 \pm 3.4) \times 10^4$	$Abs = (3.0 \pm 0.3) \times 10^{-2}\ C\ (nmol/\mu L) + (2.1 \pm 3.6) \times 10^{-2}$
Correlation coefficient	0.999	0.995
Concentration range	1.0–15.0 (mg/L)	2.0–20.0 (nmol/μL)

A area, *Abs* absorbance, *C* concentration, *HPLC* high-performance liquid chromatography, *TE* Trolox equivalents, *UV-Vis* ultraviolet-visible

[a] A is the area of the peak (HPLC method), and C is the concentration of tyrosol (μg/L) in the case of the HPLC method, *Abs* is the absorbance (UV-Vis spectrophotometer method), and C is the Trolox Equivalents (TE) concentration (nmol/μL)

[b] Mean calibration curve based on three independent calibration curves

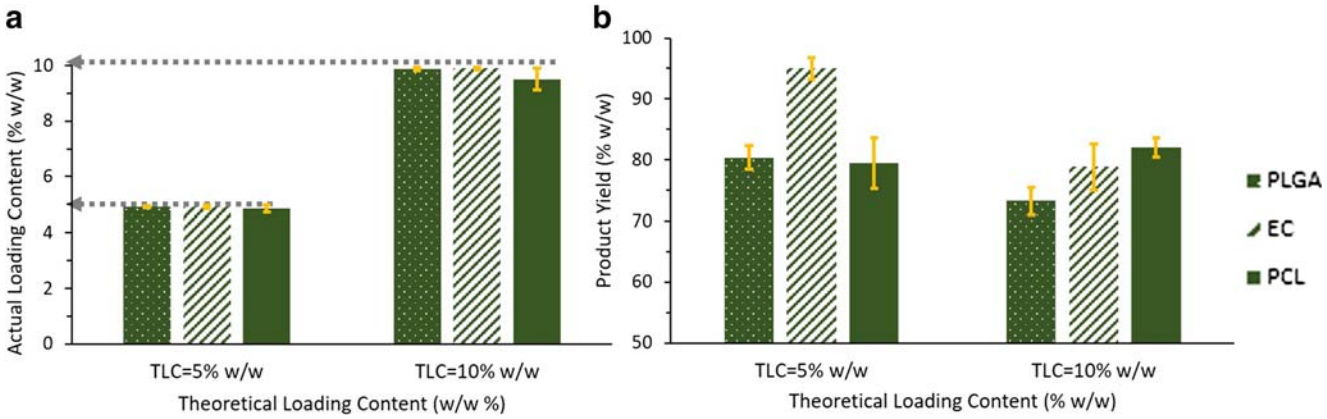

Fig. 1 Actual loading content (% *w/w*) (**a**) and product yield (% *w/w*) (**b**) of tyrosol-loaded microparticles (PLGA, poly(D,L-lactide-*co*-glycolide); EC, ethylcellulose; PCL, polycaprolactone; TLC, theoretical loading content (% *w/w*)). Data are expressed as mean ± standard deviation of three independent assays. The yellow bars correspond to the error bars based on the standard deviation of three independent assays. The arrows showed in gray refer to the TLC (% *w/w*) expected

theoretical loading content considered by the authors (theoretical loading content of pomegranate seed oil of 15%).

The phenolic compound, hydroxytyrosol, also present in high quantities in both olive oil and olive mill wastes was encapsulated in EC polymer-based systems in similar conditions to the ones reported in the present study (Paulo and Santos 2018b).

Similarly, two alternative TLCs (5% and 10% *w/w*) were studied. However, in the case of the encapsulation of hydroxytyrosol using EC as a coating material, the actual loading content was 2.2 ± 0.1% *w/w* (corresponding to 22 ± 1 mg of hydroxytyrosol encapsulated/g of dried dispersion) in the case of the TLC of 5% *w/w* and 4.9 ± 0.2% *w/w* (corresponding to 49 ± 2 mg of hydroxytyrosol encapsulated/g of dried dispersion). A decrease of around 50% was observed from the TLC to the actual loading content when hydroxytyrosol-loaded EC microparticles were produced. In the present study, the actual loading content was quite similar to the TLC against the results obtained by Paulo and Santos (2018b).

Tyrosol is structurally related to hydroxytyrosol, as their chemical structures are identical except that hydroxytyrosol holds an extra hydroxy group in meta-position (Fig. 2). The fact that hydroxytyrosol holds on the benzene moiety an extra hydroxyl group next to other hydroxyl group provides to hydroxytyrosol an ortho diphenol or catechol structure (Tuck and Hayball 2002). It is reported that the absence of this *o*-diphenol structure, in tyrosol, entails considerable differences in the compound susceptibility to oxidation as well as its antioxidant capacity and potency as chemopreventive compounds under oxidative stress conditions (Preedy and Watson 2017).

The absence of the extra hydroxy group in tyrosol is responsible for its lower aqueous solubility character when compared to hydroxytyrosol. Due to its slightly lower solubility in an aqueous system, tyrosol has a less tendency to diffuse from the internal aqueous phase (w_1) to the external aqueous phase (w_2), and therefore a higher amount of tyrosol was entrapped in the polymer matrix. In the case of hydroxytyrosol, due to its slightly higher hydrophilicity, its loss into the external aqueous phase (w_2) was promoted while the dispersed phase (w_1/o) stayed in the semi-solid/transitional state (Jyothi et al. 2010).

Moreover, another relevant factor that should be considered in the present analysis is tyrosol-polymer interaction. The slightly higher lipophilicity of tyrosol, when compared to hydroxytyrosol, is probably responsible for the higher amount of tyrosol retained in the polymers. Relative stronger interaction forces between tyrosol and the polymers probably had promoted its retention in the polymer matrices.

The yield of production was evaluated for 6 different formulations corresponding to three polymers, and two alternative TLC, for each polymer tested. All the formulations were run in triplicate in a total formulation number of 18. Only average results are presented.

The mean production yields of tyrosol-loaded PLGA microparticles with a TLC of 5% *w/w* and 10% *w/w* were 80.3 ± 1.9% *w/w* and 73.2 ± 2.2% *w/w*, respectively.

Regarding the product yield results of tyrosol-loaded EC microparticles with a TLC of 5% *w/w* and 10% *w/w* were 95.0 ± 1.7% and 78.8 ± 3.7%, respectively.

In the case of tyrosol-loaded PCL microparticles formulated considering a TLC of 5% and 10% *w/w*, the mean production yields were 79.4 ± 4.2% and 82.0 ± 1.6%, respectively.

The results of this study demonstrate that both in the case of tyrosol-loaded PLGA microparticles and tyrosol-loaded EC microparticles, the TLC affected the production yield as was

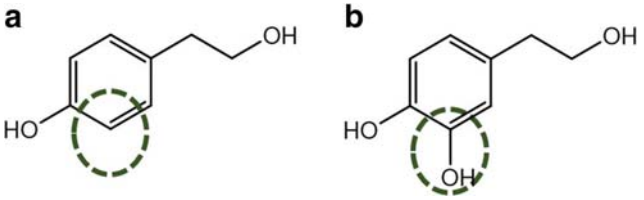

Fig. 2 Chemical structure of tyrosol (**a**) and hydroxytyrosol (**b**)

observed a statistically significant difference between the mean production yield among the TLC tested ($P = 0.01 < 0.05$, in the case of using PLGA and $P = 1.71 \times 10^{-4} < 0.05$ using EC as a coating material; significance level considered: 95%). For both polymers was verified that an increase in the TLC from 5 to 10% *w/w* led a decrease of the production yield as displayed in Fig. 3.

To the authors' best knowledge, this is the first time that is reported the encapsulation of tyrosol. Therefore, there is a lack of published data suitable for the direct comparison regarding the production yield. However, regarding the results of the encapsulation of a related compound of tyrosol—hydroxytyrosol—into EC microparticles, was also observed a significant ($P < 0.05$) decrease in the production yield from the microparticles formulated with a TLC of 5% *w/w* to the ones formulated with 10% *w/w* (Paulo and Santos 2018b).

Regarding the results of the production yield of tyrosol-loaded PCL microparticles, the production yield seemed not to be affected by the TLC as there were no observed differences between the experimental groups (grouped by the TLC) at the production yield level as the *P* value obtained was 0.38 ($P > 0.05$; confidence level of 95%).

During the study of the effects of wall materials and operating conditions on physicochemical properties of encapsulated banana passionfruit pulp by spray-drying, the authors Troya et al. (2018) found that the production yield was dependent of the inlet temperature on the spray-drier and the core to encapsulating material ratio (physicochemical feature that can be related to the theoretical loading content as an increase of the core to the encapsulation material ratio imply an increase of the theoretical loading content). Similarly to the results obtained in the present study regarding the inclusion of tyrosol into PLGA and EC polymeric systems—an increase in the loading content led to a decrease in the product yield. The obtained values by Troya et al. (2018) for the production yield (production yield ranged between 29.35 and 60.84%) differing from those obtained in the present study. Even though the chemical composition of the selected polymers and core materials, microencapsulation technique and even operating conditions, the use of the spray-dryer may limit the production yield– the operational temperature conditions restrained the mass of microparticles obtained after the microencapsulation process: when the temperature in the spray-drying chamber is too low, microparticles tend to adhere to the drying chamber and the cyclone filter wall due to the high moisture content; when the temperature is too high, microparticles tend to crack and degrade Troya et al. (2018).

The results of this study are significant as was found a lack of published data regarding the comparison of the theoretical loading content with the production yield.

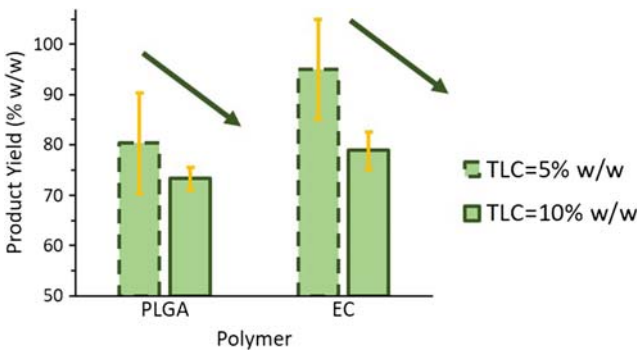

Fig. 3 Results regarding the production yield of tyrosol-loaded PLGA and EC microparticles. Two alternative TLC are presented (5% *w/w* and 10% *w/w*) (PLGA, poly(D,L-lactide-*co*-glycolic) acid; EC, ethylcellulose; TLC, theoretical loading content). The yellow bars correspond to the error bars based on the standard deviation of three independent assays

Assessment of Tyrosol Encapsulation Efficiency

The encapsulation efficiency of tyrosol-loaded microparticles was evaluated through qualitative and quantitative methods. For the qualitative evaluation of the efficient incorporation of tyrosol into polymer matrices selected for this study, the FTIR method was applied. The ATR mode of FTIR was used. It allows evaluating surface properties of the materials rather than their bulk properties. The quantitative assessment of tyrosol encapsulation efficiency into microparticles was performed as described in the "Determination of the Tyrosol Loading Content, the Encapsulation Efficiency, and the Product Yield" section and accordingly to Eq. (3).

Qualitative Assessment of Tyrosol Encapsulation Efficiency by FTIR

In the present study, the FTIR-ATR was employed in order to identify specific functional groups present in the surface of tyrosol-loaded microparticles to evaluate the effectiveness of the incorporation of this bioactive compound in different polymeric matrices.

The presence of characteristic functional groups of tyrosol which are not present in the coating materials used indicates the possibility of the adsorption of tyrosol in the surface of microparticles. If tyrosol was not efficiently incorporated in microparticles, specific FTIR bands associated with the benzene ring present in the chemical structure of tyrosol (Fig. 2a) should be observed in FTIR spectra. The characteristic FTIR bands of tyrosol are as follows: (i) the C-H stretch from 3100 to 3000 cm^{-1}, (ii) two bands related to the C=C stretch (in-ring) from 1600 to 1400 cm^{-1}, and (iii) the out of the plane bending C-H aromatic disubstituted in *para* position, from 900 to 800 cm^{-1}.

The wavenumbers (cm^{-1}) and the assignments of the bands observed in the FTIR spectra of tyrosol (TYR), PLGA, PO microparticles formulated with PLGA and tyrosol-loaded PLGA microparticles formulated considering a TLC of 5%

w/w and 10% *w/w* are presented in Table 3. Similarly, the corresponding wavenumbers (cm^{-1}) and assignments of TYR, EC, loaded (TYR-EC TLC = 5% and TYR-EC TLC = 10%), and PO microparticles (PO-EC MPs) are presented in Table 4. Similar assignments using PCL as the polymer-carrier are presented in Table 5.

The signature peaks of tyrosol, related to the presence of an aromatic structure, are highlighted in gray in Tables 3, 4, and 5. These signature peaks include the ones related to (i) the C-H aromatic, stretching vibration mode at 3130 cm^{-1}, (ii) the C-H aromatic disubstituted in *para* position bending out of the plane at 815 cm^{-1}, and (iii) two bands related to the C=C aromatic stretching vibration at 1510 cm^{-1} and at 1450 cm^{-1}. The characteristic peaks of tyrosol were not observed in loaded microparticles. The wavenumber corresponding to the C-O stretching vibrational mode of tyrosol is present in the fingerprint area (FPA), and more importantly, it is a characteristic band for all the polymers understudy, so it was not considered for the quantitative detection of tyrosol at the surface of loaded microparticles.

The signature peaks of PLGA, PO microparticles formulated with PLGA and tyrosol-loaded PLGA microparticles formulated considering two alternative TLC (5% *w/w* and 10% *w/w*) are similar (Table 3) and do not present any relevant similarity with the signature peaks of tyrosol. Analogous results were obtained with EC (Table 4) and PCL (Table 5) when they were used as coating materials of tyrosol. For all the polymers studied, significant band shiftings were not observed in the FTIR spectra of loaded microparticles when compared to the spectra of PO microparticles. These observations confirm the efficient incorporation in PLGA, EC, and PCL micro-systems as were not found any of the signature peaks of tyrosol in loaded microparticles.

To the authors' best knowledge, this is the first time that is reported the encapsulation of tyrosol in alternative polymer-carriers. Therefore, there is a lack of published data regarding the FTIR studies of tyrosol encapsulated in polymeric matrices suitable for direct comparison.

However, it is reported that using the same encapsulation technique ($w_1/o/w_2$ solvent evaporation technique), similar formulation and process conditions, is possible to achieve efficient incorporation of the selected bioactive compound. According to Paulo and Santos (2018b), hydroxytyrosol, a similar compound to tyrosol, was efficiently encapsulated using EC as the polymer coating material.

Quantitative Assessment of Tyrosol Encapsulation Efficiency

The quantitative assessment of tyrosol encapsulation efficiency was evaluated considering Eq. (3) and as described in the "Determination of the Tyrosol Loading Content, the Encapsulation Efficiency, and the Product Yield" section. The graphical representations of tyrosol encapsulation efficiency for each polymer-carrier studied (PLGA, EC, and PCL) and for each TLC are presented in Fig. 4.

The mean tyrosol encapsulation efficiency of loaded microparticles formulated considering a TLC of 5% *w/w* were 99.1 ± 0.3% *w/w* for tyrosol-loaded PLGA microparticles, 99.3 ± 0.5% *w/w* for tyrosol-loaded EC microparticles, and 99.1 ± 0.1% *w/w* in the case of for tyrosol-loaded PCL microparticles.

The mean tyrosol encapsulation efficiency of tyrosol-loaded PLGA, EC, and PCL microparticles, considering a

Table 3 Wavenumbers (cm^{-1}) and assignments for the bands observed in the FTIR spectra of TYR, PLGA, PO-PLGA microparticles and loaded microparticles considering a TLC of 5% *w/w* (TYR-PLGA MPs TLC = 5%) and a TLC of 10% *w/w* (TYR-PLGA MPs TLC = 10%)

Bond type	Chemical functional group	Vibration mode	Wavenumber (cm^{-1})				
			TYR	PLGA	PO-PLGA MPs	TYR-PLGA MPs (TLC = 5%)	TYR-PLGA MPs (TLC = 10%)
O-H	–	Stretching	3382	3496	NF	NF	NF
C-H	Alkanes	Stretching	2879	2997 2950	2997 2951	2997 2951	2297 2945
	$-CH_2-$	Bending	1450	1384	1384	1385	1392
	$-CH_3$		–	1452	1429	1429	1429
	Aromatic	Stretching	3130	–	–	–	–
	Aromatic, disubstituted, *para* position	Bending out-of-plane	815	–	–	–	–
C=C	Aromatic	Stretching	1510 1450	–	–	–	–
C-O	Esters, alcohols and carboxylic acids	Stretching	FPA	1166 1085	1162 1086	1167 1085	1167 1085
C=O	Esters and carboxylic acids	Stretching	–	1751	1747	1749	1749

FPA fingerprint area, *MP* microparticle, *NF* not found, *PLGA* poly(D,L-lactide-*co*-glycolic) acid, *PO* polymer only, *TLC* theoretical loading content (*% w/w*), *TYR* tyrosol

Table 4 Wavenumbers (cm^{-1}) and assignments for the bands observed in the FTIR spectra of TYR, EC, PO-EC, and loaded microparticles considering a TLC of 5% *w/w* (TYR-EC MPs TLC = 5%) and a TLC of 10% (TYR-EC MPs TLC = 10%)

Bond type	Chemical functional group	Vibration mode	Wavenumber (cm^{-1})				
			TYR	EC	PO-EC MPs	TYR-EC MPs (TLC = 5%)	TYR-EC MPs (TLC = 10%)
O-H	–	Stretching	3382	3460	3470	3470	3470
C-H	Alkanes	Stretching	2879	2867	2867	2868	2867
	$-CH_2-$	Bending	1450	FPA	FPA	FPA	FPA
	$-CH_3$		–	1375	1375	1375	1375
	Aromatic	Stretching	3130	–	–	–	–
	Aromatic, disubstituted, *para* position	Bending out-of-plane	815	–	–	–	–
C=C	Aromatic	Stretching	1510 1450	–	–	–	–
C-O-C	Aliphatic ether	Stretching	FPA	1051	1055	1055	1055

EC ethyl cellulose, *FPA* fingerprint area, *MP* microparticle, *PO* polymer only, *TLC* theoretical loading content (% *w/w*), *TYR* tyrosol

TLC of 10% *w/w* were 98.7 ± 0.5% *w/w*, 98.5 ± 1.0% *w/w*, and 98.9 ± 0.1% *w/w*, respectively.

In the case of tyrosol-loaded PLGA and EC microparticles, the tyrosol encapsulation efficiency was not affected by the TLC as was not observed statistically significant differences among the two experimental groups (TLC of 5% *w/w* and TLC of 10% *w/w*) for each polymer, considered individually as the *P* value was higher than 0.05, considering a significance level of 95% ($P = 0.32$ in the case of tyrosol-loaded PLGA microparticles and $P = 0.26$ in the case of loaded EC microparticles). The tyrosol loss during the encapsulation was only 0.9 ± 0.3% *w/w* and 1.3 ± 0.5% *w/w* in the case of PLGA-loaded microparticles formulated considering 5% and 10% *w/w* of the TLC, respectively. The tyrosol loss during the microencapsulation procedure of tyrosol-loaded EC microparticles was 0.7 ± 0.5% *w/w* and 1.5 ± 1.0% *w/w*, for a TLC of 5% *w/w* and 10% *w/w*, respectively.

The results regarding the tyrosol encapsulation efficiency of tyrosol-loaded PCL microparticles were dissimilar to the ones obtained for tyrosol-loaded PLGA and EC microparticles. The encapsulation efficiency in the biocompatible polymer PCL was affected by the theoretical loading content as, considering a confidence level of 95%, the null hypothesis (H_0: tyrosol encapsulation efficiency is not affected by the TLC value) was not verified ($P = 0.01 < 0.05$). The total amount of tyrosol lost during the encapsulation process was 9 ± 1 mg of tyrosol/g of tyrosol used for the formulation in the case of a TLC of 5% *w/w* and 11 ± 1 mg tyrosol/g of tyrosol used for the formulation in the case of a TLC of 10% *w/w*.

In this case, the increase of the TLC led to a decrease of tyrosol encapsulation efficiency. Similar trends were also observed by other authors as Freytag et al. (2000) and Paulo and Santos (2018b).

Table 5 Wavenumbers (cm^{-1}) and assignments for the bands observed in the FTIR spectra of TYR, PCL, PO-PCL, and loaded microparticles considering a TLC of 5% *w/w* (TYR-PCL MPs TLC = 5%) and a TLC of 10% (TYR-PCL MPs TLC = 10%)

Bond type	Chemical functional group	Vibration mode	Wavenumber (cm^{-1})				
			TYR	PCL	PO-PCL MPs	TYR-PCL MPs (TLC = 5%)	TYR-PCL MPs (TLC = 10%)
C-H	Alkanes	Stretching	2879	2943 2868	2943 2868	2943 2868	2943 2868
	$-CH_2-$	Bending	1450	FPA	FPA	FPA	FPA
	$-CH_3$		–	1361	1361	1361	1361
	Aromatic	Stretching	3130	–	–	–	–
	Aromatic, disubstituted, *para* position	Bending out-of-plane	815	–	–	–	–
C=C	Aromatic	Stretching	1510 1450	–	–	–	–
C-O-C	Aliphatic ether	Stretching	FPA	1107	1106	1107	1107
C=O	Ester	Stretching	–	1726	1726	1726	1726

FPA fingerprint area, *MP* microparticle, *PCL* polycaprolactone, *PO* polymer only, *TLC* theoretical loading content (% *w/w*), *TYR* tyrosol

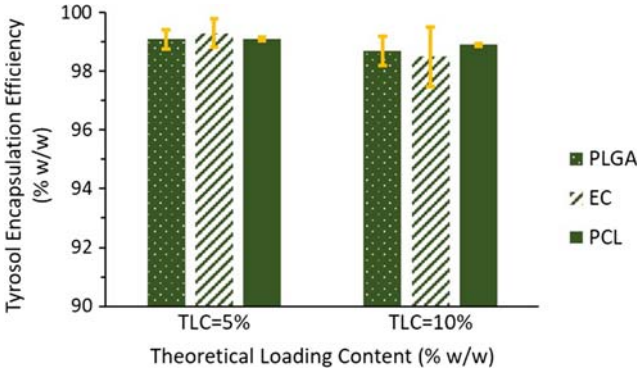

Fig. 4 Tyrosol Encapsulation Efficiency (% w/w) of tyrosol-loaded microparticles (PLGA - poly(D,L-lactide-co-glycolide); EC - ethylcellulose; PCL – polycaprolactone; TLC – Theoretical Loading Content (% w/w)); Data are expressed as mean ± standard deviation of three independent assays; The yellow bars correspond to the error bars based on the standard deviation of three independent assays

Comparing the results obtained when hydroxytyrosol was encapsulated in EC polymer-based system considering two alternative TLC (5% *w/w* and 10% *w/w*) (Paulo and Santos 2018b), a related pattern was observed, in the present study, an increase in TLC from 5 to 10% *w/w*, resulted in a decrease in the encapsulation efficiency.

Similarly to the results obtained by Troya et al. (2018) and even though that the encapsulating and core materials, and microencapsulation technique applied were dissimilar, the authors verified that an increase of the core to the encapsulating material ratio and therefore the theoretical loading content led to a decrease of the encapsulation efficiency.

The reported observation can be explained by the fact that when microparticles are loaded with higher amount of tyrosol, probably a higher flux of tyrosol may occur when microparticles are in the semi-solid state (Gabor et al. 1999; Krishnamachari et al. 2007; Paulo and Santos 2018b).

The results regarding the quantitative assessment of the encapsulation efficiency are fairly significant. For all polymer-carriers was observed high encapsulation efficiency values. In the case of using PLGA or even EC as polymer-carriers, the encapsulation efficiency was independent of the TLC. Differently, when PCL is used as the coating material, the TLC seemed to affect the encapsulation efficiency. This observation should be carefully considered when is intended the coating of tyrosol in a PCL polymer-based system, and its incorporation in food matrices—a compromise between the encapsulation efficiency and a load of tyrosol should be considered.

DSC Analysis

The efficient incorporation of tyrosol in PLGA, EC, and PCL microsystems can be indirectly confirmed by DSC analysis. The comparison of the thermal stability of the encapsulated forms of tyrosol (tyrosol-loaded microparticles) with the free form (tyrosol standard) allows to indirectly confirm the adequate incorporation of this bioactive compound in the selected polymer matrices (Hill et al. 2013; Karathanos et al. 2007). Moreover, the analyses of DSC thermograms allow characterizing the physicochemical status of the bioactive compound formulated into microparticles (Dubernet 1995; Zhang and Gao 2007).

From the DSC thermograms analysis (Fig. 5a), pure tyrosol presents a sharp endotherm peak at 95 °C (correspondent area of 173.8 J/g) corresponding to the melting point of the pure compound. In a research, regarding the coupling of tyrosol, quercetin or ferulic acid and electron beam irradiation to cross-link chitosan-gelati films, Benbettaïeb et al. (2015) reported that the melting point of tyrosol is ranged between 89 and 92 °C, as predicted values from ACD/Labs software from Chemspider and PubChem. However, to the authors' best knowledge, this is the first time that is performed a DSC analysis of tyrosol. The obtained value is relatively close to the range presented by Benbettaïeb et al. (2015); nevertheless, the purity degree may contribute significantly to the melting point value obtained—98% of the analyzed solid corresponded to pure tyrosol. Impurities (about 2%) present in the sample may be the explanatory reason for the obtained melting point value slightly above the predicted range values.

Concerning the DSC results of tyrosol-loaded PLGA microparticles, the absence of the melting endotherm peak of tyrosol at 95 °C yield some evidence of the efficient incorporation of tyrosol in PLGA microparticles as the melting points tends to shift or disappear when during the incorporation of a bioactive compound in a polymer-based system. Any of the crystalline tyrosol material in microparticles was not detected in the DSC study of tyrosol-loaded PLGA microparticles. Therefore, it can be concluded that tyrosol was incorporated in PLGA shells in an amorphous or disordered-crystalline phase of a molecular dispersion or a solid solution state in PLGA matrices after microparticle production. Similar results were obtained by Zhang and Gao (2007) when they encapsulated temozolomide drug into PLGA microparticles intended for antitumor activity studies against Glioma C6 cancer cells.

According to Friess and Schlapp (2002), the glass-transition temperature (T_g) of PLGA polymers ranges between 40 and 65 °C, increasing with the increase on the molecular weight. In the present study, the T_g value of PLGA was found to be 53 °C (Resomer® RG 504, lactide/glycolide 50/50) corresponding to an area of 8 J/g. The DSC thermograms of tyrosol-loaded PLGA microparticles formulated considering a TLC of 5% *w/w* and 10% *w/w* present an endotherm sharp peak at 53 °C (area of 11 J/g) and 54 °C (correspondent area of 8 J/g), respectively. As no significant changes were found on the T_g value of tyrosol-loaded PLGA microparticles compared to PLGA, it corroborates the hypothesis of the incorporation of tyrosol into PLGA microparticles on its amorphous form (Mandal et al. 2002; Pamujula et al. 2004, 2008; Paulo and Santos 2018b).

Regarding the DSC results of tyrosol-loaded EC microparticles, it can be stated that the absence of a sharp endotherm peak between 70 and 120 °C, relative to the tyrosol melting point at 95 °C indicates the efficient incorporation of tyrosol in EC polymer matrices. The mid T_g value of EC was found to be 122 °C, whereas the T_g values of tyrosol loaded EC microparticles formulated considering a TLC of 5% *w/w* and 10% *w/w* were found to be 150 °C and 138 °C. There was verified a shift on the T_g value from EC to higher values when tyrosol was encapsulated using EC as a shell material. In the case of tyrosol-loaded microparticles were observed shifts of the T_g value position of the polymer due to anti-plasticizing effects of the active ingredient. Moreover, the endotherm peak of tyrosol is not present in the DSC thermograms; therefore, tyrosol and EC formed a solid solution. A similar result was obtained by Paulo and Santos (2018b): solid solutions due to anti-plasticizing effects were obtained when hydroxytyrosol was encapsulated using EC as a coating material.

Respecting the DSC analysis of tyrosol-loaded PCL microparticles as well as only PCL, it was verified that the melting endotherm peak of PCL (found to be 64 °C) was the absence of tyrosol-loaded PCL microparticles. Tyrosol-loaded PCL microparticles endotherm peaks were found to be 60 °C in the case of microparticles formulated considering a TLC of 5% *w/w* and 95 °C, in the case of microparticles formulated considering a TLC of 10% *w/w*. In the case of tyrosol-loaded PCL microparticles, alternative thermal behaviors were found between the samples prepared considering a TLC of 5% *w/w* and 10% *w/w*. In the case of tyrosol-loaded microparticles formulated considering 5% *w/w* of TLC, the endotherm peak of tyrosol is not present in the DSC thermogram of tyrosol-loaded PCL microparticles (TLC of 5% *w/w*; Fig. 5d) and was observed a shift on the T_g of PCL to lower temperatures indicating that tyrosol formed a solid solution with PCL due to plasticizing effects. In the case of tyrosol-loaded microparticles formulated considering a TLC of 10% *w/w*, tyrosol was encapsulated on its crystalline form as the $T_g$of tyrosol-loaded PCL microparticles (TLC = 10% *w/w*) was found to be close to the T_g value of tyrosol (actual value found for loaded microparticles of 95 °C). The obtained results are similar to some found by other authors. Natarajan et al. (2011) found a similar value for the T_g of PCL (61 °C) when they were formulating microspheres containing quercetin for the treatment of rheumatoid arthritis. A similar value (69 °C) for the melting point of PCL was also presented by Nagy et al. (1999) when they were characterizing blends of PCL with polyvinyl alcohol. Also, Dasaratha and Sathyamoorthy (2018) found the melting temperature of PCL at 63 °C when they were preparing etoposide-loaded PCL microspheres by solvent evaporation technique. The results found in the literature are in agreement with the ones obtained in the present study.

The typical events that may occur when a bioactive ingredient is encapsulated in a polymer matrix are of 3 different types as follows: (i) the bioactive ingredient form with the polymer a solid solution and consequently the melting endotherm peak of the encapsulated material is not present in the thermogram of loaded microparticles, and there is verified a shift of the T_g of the polymer to higher (anti-plasticizing effects) or to lower (due to plasticizing effects) temperatures; (ii) the bioactive ingredient is dispersed in the polymer matrix in its amorphous form, therefore, the T_g of the polymer is not changed, and the melting endotherm peak of the bioactive compound is not shown on the thermogram of loaded microparticles; and (iii) the bioactive compound is incorporated in the polymer matrix in its crystalline form and, in this case, neither the T_g value of the polymer and the bioactive compound are changed (Mandal et al. 2002; Pamujula et al. 2004, 2008; Paulo and Santos 2018a). However, in case (ii), the absence of the melting peak of the bioactive ingredient may not be detected due to the dispersion of a low amount of bioactive compound in the polymeric matrix as described by Natarajan et al. (2011).

The DSC results of tyrosol-loaded microparticles are significant. The pure compound presents its melting point at 95 °C. In the case of tyrosol-loaded PLGA microparticles for both TLC, considered tyrosol was incorporated in PLGA on its amorphous form, contrasting with tyrosol-loaded EC microparticles as tyrosol formed a solid solution with EC at both TLCs considered. Distinctively, tyrosol-loaded PCL microparticles formulated considering alternative TLCs presented different thermal behaviors: when a TLC of 5% *w/w* was considered, tyrosol formed a solid solution (due to plasticizing effects) with PCL, however, when it was considered a TLC of 10% *w/w*, tyrosol was incorporated in PCL matrix on its crystalline form, indicating, therefore, that tyrosol kept its crystallinity until the degradation of tyrosol-loaded PCL microparticles (TLC = 10% *w/w*).

TGA

The TGA thermograms and the derivative thermogravimetry (DTG) thermograms from 30 to 810 °C of tyrosol, powders of loaded microparticles (tyrosol-loaded PLGA microparticles, tyrosol-loaded EC microparticles, and tyrosol-loaded PCL microparticles at two different TLCs—5% *w/w* and 10% *w/w*) and polymers (PLGA, EC, and PCL) are presented in Fig. 6a, b, respectively.

These thermogravimetric analyses were performed to evaluate the weight change of microparticles with temperature. The weight loss extent of formulations was similar in similar temperature ranges, excluding the TGA thermogram of pure tyrosol. Both pure tyrosol, polymers (PLGA, EC, and PCL) and the powders of loaded microparticles presented only one level of weight loss.

According to Yoksan et al. (2010), the peaks on the DTG thermogram (Fig. 6b) corresponds to the highest rate of

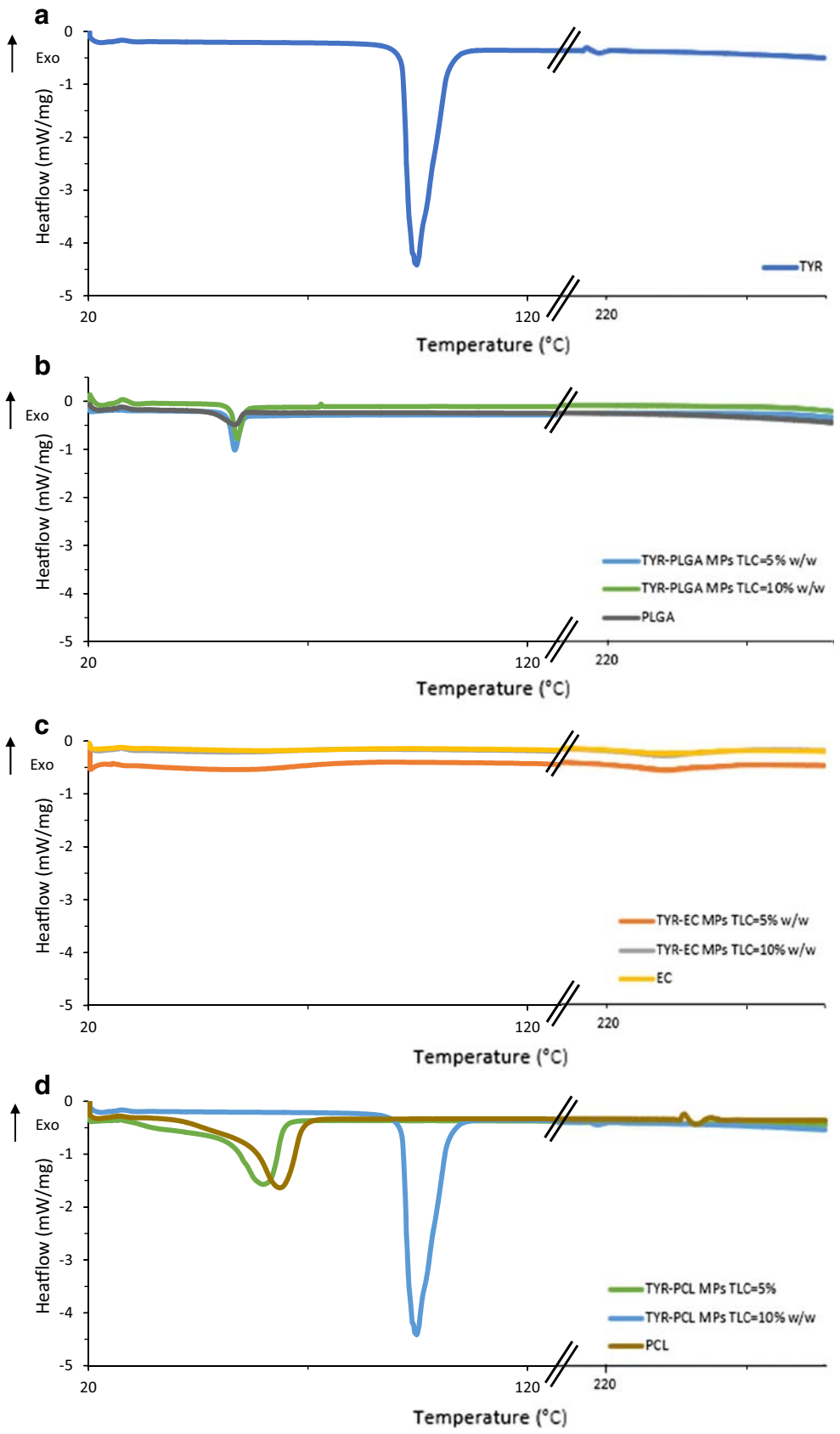
a
Exo
Heatflow (mW/mg)
0
-1
-2
-3
-4
-5
20
120
220
Temperature (°C)
TYR
b
Exo
Heatflow (mW/mg)
Temperature (°C)
TYR-PLGA MPs TLC=5% w/w
TYR-PLGA MPs TLC=10% w/w
PLGA
c
Exo
Heatflow (mW/mg)
Temperature (°C)
TYR-EC MPs TLC=5% w/w
TYR-EC MPs TLC=10% w/w
EC
d
Exo
Heatflow (mW/mg)
Temperature (°C)
TYR-PCL MPs TLC=5%
TYR-PCL MPs TLC=10% w/w
PCL

◀ **Fig. 5** Differential scanning calorimetry thermograms of pure tyrosol (**a**), tyrosol-loaded PLGA microparticles (**b**), tyrosol-loaded EC microparticles (**c**), and tyrosol-loaded PCL microparticles (**d**) (EC, ethylcellulose; MPs, microparticles; PCL, polycaprolactone; PLGA, poly(D,L-lactide-*co*-glycolide; TYR, tyrosol)

weight loss and therefore to the degradation temperature (T_d) of the component in the analyzed material. The weight loss of tyrosol happened in the range of 132 to 237 °C (Fig. 6a). The analysis of the DTG thermogram of tyrosol revealed that tyrosol was degraded at 230 °C (Fig. 6b).

The interpretation of TGA and DTG thermograms of tyrosol-loaded PLGA indicate that the weight loss change occurred in the range of 265 to 381 °C, corresponding to a T_d of 330 °C in the case of tyrosol-loaded PLGA microparticles formulated considering a TLC of 5% *w/w* and the weight loss occurred in the range of 261 °C to 381 (T_d of 343 °C), in the case of microparticles formulated considering a TLC of 10% *w/w*. It was observed a shift to higher temperatures of the T_d when PLGA was loaded with 5 to 10% *w/w*. These results are significant as tyrosol-loaded PLGA microparticles formulated with a higher loading presented higher thermogravimetric stability than microparticles formulated considering a TLC of 5% *w/w*.

When EC was used as a polymer-carrier, the weight loss change occurred in the range of 287 °C and 401 °C associated with a T_d of 306 °C in the case of loaded EC microparticles formulated with a TLC of 5% *w/w*; in the case of tyrosol-loaded EC microparticles associated with TLC of 10% *w/w*, the weight loss occurred between 303 and 397 °C (T_d at 363 °C). It was verified a shift in the T_d value from 306 to 363 °C when the TLC was increasing from 5 to 10% *w/w*. An increase of the loading content led to an increase in the thermogravimetric stability of microparticles. A similar conclusion was drawn when hydroxytyrosol was encapsulated using the same polymer-carriers (EC) and considering the TLC of 5% *w/w* and 10% *w/w* (Paulo and Santos 2018a).

Regarding the analysis of TGA and DTG thermograms of tyrosol-loaded PCL microparticles, the weight loss change of loaded PCL microparticles considering a TLC of 5% *w/w* occurred between 330 and 467 °C, associated to a T_d at 412 °C. Regarding the weight loss change of tyrosol-loaded PCL, microparticles formulated considering a TLC of 10% *w/w*, it was observed between 304 and 437 °C (T_d of 412 °C). Even though, as opposed to obtained results for tyrosol-loaded PLGA and EC microparticles, with PCL was not verified a shift in the T_d to higher values with the increase of the loading content. However, PCL seemed to be the polymer to better guaranty the thermogravimetric stability of tyrosol-loaded microparticles as with PCL the weight loss change started to occur at higher temperatures (specifically in the case of tyrosol-loaded PCL microparticles formulated considering

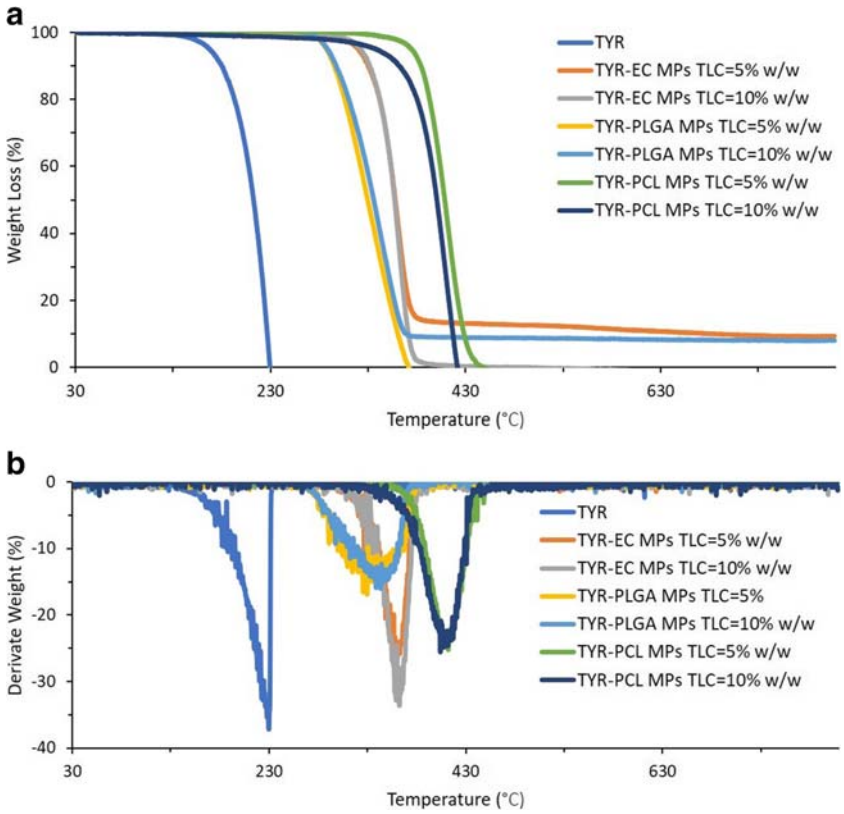

Fig. 6 Thermogravimetric analysis thermograms of different samples pure tyrosol, tyrosol-loaded PLGA microparticles, tyrosol-loaded EC microparticles, and tyrosol-loaded PCL microparticles (TGA versus temperature (**a**) and DTG versus temperature (**b**)) (EC, ethylcellulose; MPs, microparticles; PCL, polycaprolactone; PLGA, poly(D,L-lactide-*co*-glycolide; TYR, tyrosol)

a TLC of 5% *w*/*w*) and the T_d value was found to be the highest. Therefore, it can be concluded that PCL is an excellent polymer-carrier for tyrosol regarding the thermogravimetric stability of microparticles. Nevertheless, it can be stated that generally, tyrosol-loaded microparticles were nearly thermogravimetrically stable in the temperature range of 30 °C to 261 °C (the minimum value temperature found for the onset temperature—the case of tyrosol-loaded PLGA microparticles formulated considering a TLC of 10% *w*/*w*).

Comparing the DTG (Fig. 6b), thermograms were not detected significant differences in the mass loss at the beginning of the study (lower temperatures). Therefore, it can be concluded that free tyrosol molecules did not arrange on the surface of the microparticles; otherwise, a significant weight loss should have occurred in the initial stages of the process (around the degradation temperature of tyrosol), and differences in the TGA thermograms would be detectable. Moreover, it can be stated that no residual solvents were present in all the powders, as no weight loss (corresponding to ramps in the TGA thermograms or peaks in DTG thermograms) was distinguishable at low temperatures.

Evaluation of the Morphology

The scanning electron microscopy (SEM) was used to evaluate the main morphological characteristics of the powders obtained.

Microphotographs of tyrosol-loaded PLGA, EC and PCL microparticles are displayed in Fig. 7 (Fig. 7a—tyrosol-loaded PLGA microparticles considering a TLC of 5% *w*/*w*; Fig. 7b—tyrosol-loaded EC microparticles considering a TLC of 5% *w*/*w*; Fig. 7c—tyrosol-loaded PCL microparticles considering a TLC of 5% *w*/*w*; Fig. 7d—tyrosol-loaded PLGA microparticles considering a TLC of 10% *w*/*w*; tyrosol-loaded EC microparticles considering a TLC of 10% *w*/*w*; tyrosol-loaded PCL microparticles considering a TLC of 10% *w*/*w*). Microphotographs are presented with a magnification of 5000 times. Regardless of the loading content and the polymer-carrier, generally, the obtained microparticles present a smooth surface with almost no pores, fissures, or cracks. Moreover, the obtained microparticles present a spherical shape.

This type of outer topography seems to be characteristic of microparticles obtained by $w_1/o/w_2$ double emulsion solvent evaporation technique.

Similar microphotographs of loaded PLGA microparticles and PO microparticles using PLGA are displayed in the study

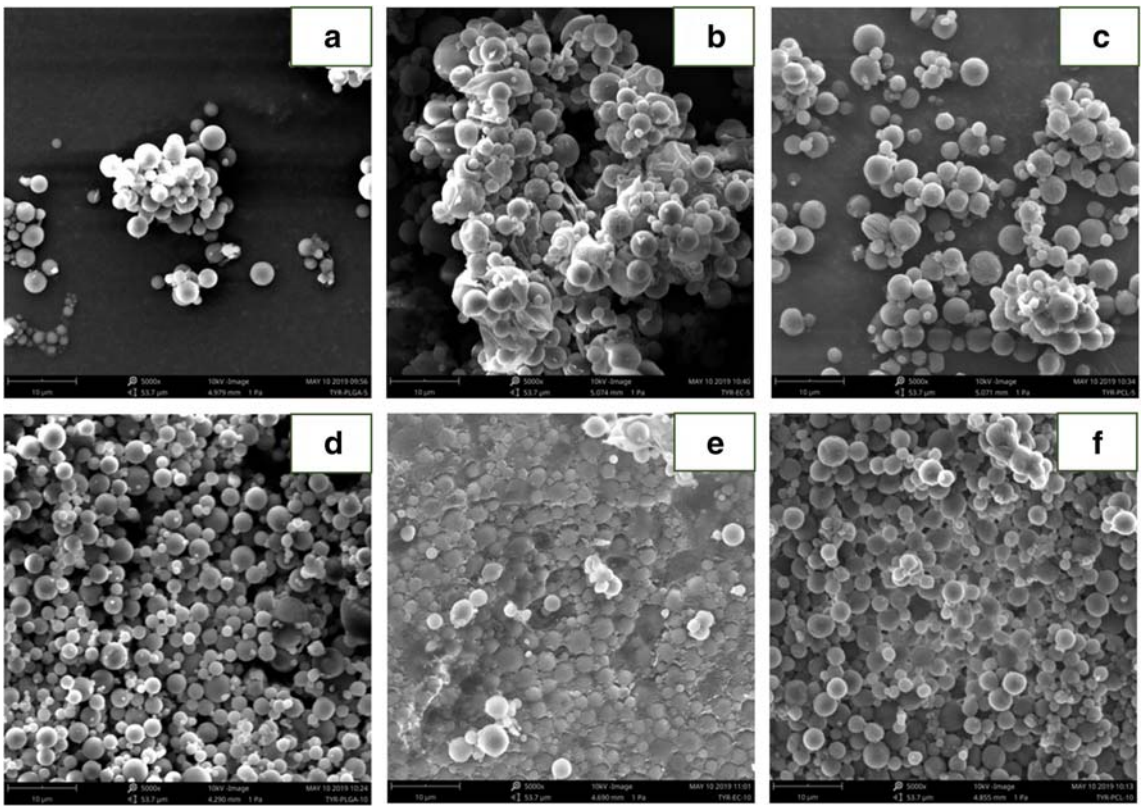

Fig. 7 Microphotographs of tyrosol-loaded PLGA microparticles considering a TLC of 5% *w*/*w* (**a**) and 10% *w*/*w* (**d**), tyrosol-loaded EC microparticles formulated considering a theoretical loading content of 5% *w*/*w* (**b**) and 10% *w*/*w* (**e**) and tyrosol-loaded PCL microparticles considering a theoretical loading content of 5% *w*/*w* (**c**) and 10% *w*/*w* (**f**) (amplification of 5000 times is presented in all microphotographs; beam intensity of 10.00 kV)

presented by Ling et al. (2008) when they encapsulated bovine serum albumin in PLGA polymer matrices by double emulsion solvent evaporation technique. The outer morphological characteristics of tyrosol-loaded PLGA microparticles exhibited in the present study (Fig. 7a, b) are almost indistinguishable from those presented by Ling et al. (2008) at the 0 weeks of degradation morphological analysis.

Identical outer morphological characteristics were found between the tyrosol-loaded EC microparticles (Fig. 7b, e) obtained in this study and the ones presented by Paulo and Santos (2018b) during the encapsulation of hydroxytyrosol into EC polymer matrices using similar formulation and operational conditions to the ones reported in the present study.

Polymer only microparticles using PCL as the coating material were produced by $w_1/o/w_2$ (Ibraheem et al. 2014). The obtained PCL coated microparticles obtained by Ibraheem et al. (2014) present a similar outer morphology to the obtained ones in the present study (tyrosol-loaded PCL microparticles; Fig. 7c, f).

Comparing the microphotographs obtained for all the polymers, an increase in the loading content led to an increase in the agglomeration degree of microparticles. From Fig. 7a (tyrosol-loaded PLGA microparticles formulated considering a TLC of 5% *w/w*) to Fig. 7b (tyrosol-loaded PLGA microparticles formulated considering a TLC of 10% *w/w*) is detectable an increase on the agglomeration degree. Similar conclusions can be drawn for both tyrosol-loaded EC and PCL microparticles.

Evaluation of the Particle Size Distribution

The particle size distribution of tyrosol-loaded PLGA, EC, and PCL microparticles are presented in Fig. 8 (differential volume (%) versus mean particle size (μm)).

Considering a TLC of 5% *w/w*, the mean particle size was 2.3 ± 0.1 μm, 2.3 ± 0.1 μm, and 7.5 ± 1.5 μm for tyrosol-loaded PLGA, EC, and PCL microparticles, respectively.

The mean particle size of tyrosol-loaded microparticles formulated considering a TLC of 10% *w/w* were 3.4 ± 0.1 μm for tyrosol-loaded PLGA microparticles, 8.8 ± 0.7 μm for tyrosol-loaded EC microparticles, and 7.8 ± 1.9 μm, in the case of tyrosol-loaded PCL microparticles.

Regarding the results of the mean particle size of tyrosol-loaded PLGA microparticles and tyrosol-loaded EC microparticles, the mean particle size seemed to be affected the loading content chosen as were observed statically significant differences between the experimental groups (for each polymer, grouped by the TLC) as the P values obtained were $P = 2.62 \times 10^{-4}$ and $P = 7.81 \times 10^{-5}$, in the case of tyrosol-loaded PLGA microparticles and tyrosol-loaded EC microparticles, respectively (confidence level considered of 95%).

Considering the results of the mean particle size of tyrosol-loaded PCL microparticles, the mean particle size seemed not to be affected by the loading content as were not observed significant differences between the two TLCs tested for each polymer as the P value obtained was higher than 0.05 ($P = 0.84 > 0.05$; confidence level of 95%).

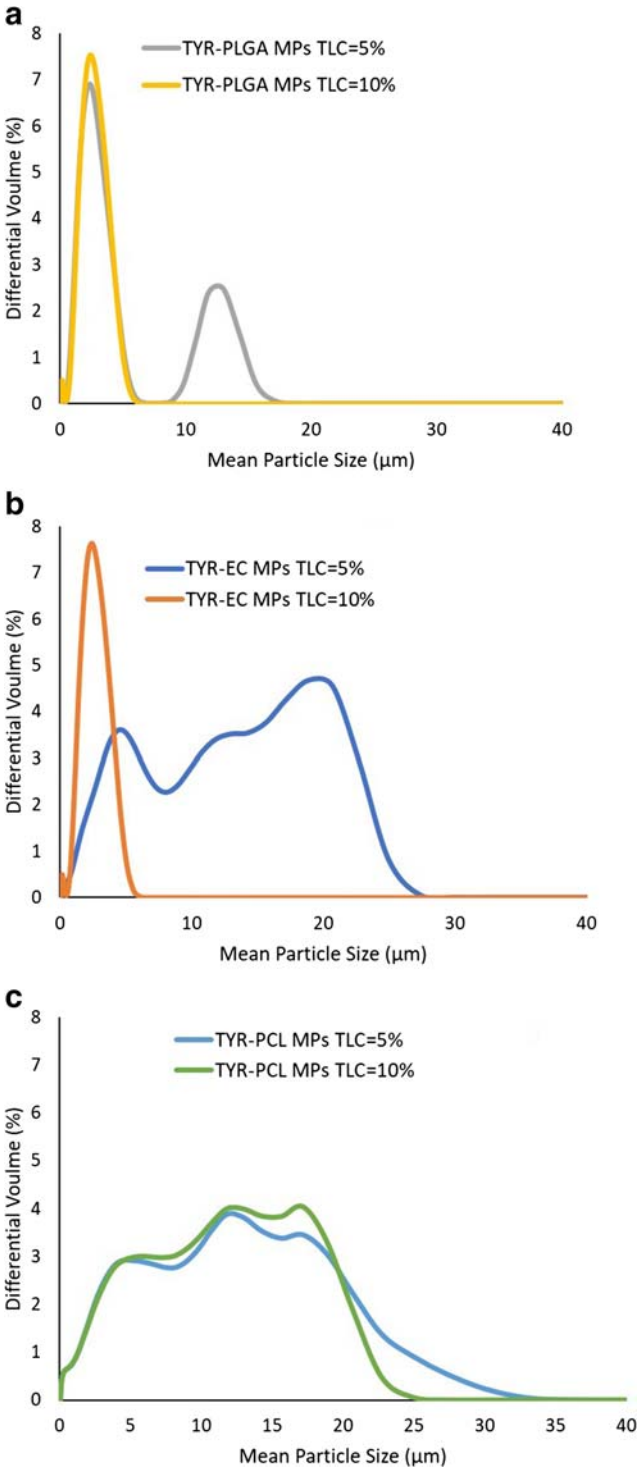

Fig. 8 Mean particle size distribution of tyrosol-loaded PLGA microparticles (**a**), tyrosol-loaded EC microparticles (**b**), and tyrosol-loaded PCL microparticles (**c**) (EC, ethylcellulose; MPs, microparticles; PCL, polycaprolactone; PLGA, poly(D,L-lactide-co-glycolide; TYR, tyrosol)

In the case of the encapsulation of tyrosol using PLGA or EC as coating materials, an increase of the loading content led to an increase of the mean particle size. Considering a TLC of 10% *w/w*, more amount of tyrosol was encapsulated, which resulted in the recovery of larger microparticles. Microparticute systems consisted of budesonide-loaded PLGA microparticles were produced by Krishnamachari et al. (2007). The authors of this research also observed that an increase in the loading content led to an increase in the mean particle size. A similar trend was also observed by Paulo and Santos (2018b) during the encapsulation of tyrosol in EC microparticulate system: an increase of the TLC from 5 to 10% *w/w* led to increasing of the mean particle size from 156.6 ± 6.9 to 304.0 ± 16.0 μm.

Regarding the graphical representation of differential volume versus the mean particle size (μm), tyrosol-loaded PLGA microparticles formulated with a TLC of 5% *w/w* presented a unimodal particle size distribution (Fig. 8a) whereas tyrosol-loaded PLGA microparticles present a bimodal particle size distribution. Similar considerations can be drawn from tyrosol-loaded EC microparticles: microparticles formulated with a TLC of 5% *w/w* present a unimodal particle distribution whereas microparticles formulated considering a TLC of 10% *w/w* present a multimodal particle size distribution. However, the results regarding the particle size distribution of tyrosol-loaded PCL microparticles, for both TLCs, the particle size distributions were multimodal. These results are in agreement to the ones obtained for the statistical significance of the influence of the TLC in the mean particle size: both tyrosol-loaded PLGA and EC microparticles mean particle sizes are affected by the TLC, and they present a unimodal particle size distribution in the case of TLC of 5% *w/w* and a bimodal or multimodal particle size distribution in the case of a TLC of 10% *w/w*. Contrastingly, tyrosol-loaded PCL microparticles mean particle size is shown to be independent of the TLC chose ($P = 0.84 > 0.05$), and it was observed for both TLCs, a multimodal particle size distribution (Fig. 8c).

Comparative results were obtained by Paulo and Santos (2018b) as was noticed a unimodal particle size distribution when was considering a TLC of hydroxytyrosol of 5% *w/w* and a bimodal particle size distribution when a TLC of 10% *w/w* was considered.

Regarding the results of polydispersity, the mean polydispersity values were obtained according to Eq. (4) and as described in "Evaluation of the Particle Size Distribution" section.

Tyrosol-loaded PLGA microparticles formulated with a TLC of 5% *w/w* and 10% *w/w* presented a mean PDI of 1.3 ± 0.1 and 1.8 ± 0.3, respectively. In the case of microparticles coated with EC, the mean PDI values obtained were 1.3 ± 0.1 and 3.0 ± 0.2 for the TLC of 5% *w/w* and 10% *w/w*, respectively. Tyrosol-loaded PCL microparticles presented mean PDI values of 2.7 ± 0.2 and 2.9 ± 0.3 for a TLC of 5% *w/w* and 10% *w/w*, respectively.

Only tyrosol-loaded EC microparticles PDI seemed to be affected by the TLC as the *P* value obtained was $P = 4.00 \times 10^{-5} < 0.05$. In the case of microparticles produced using PLGA and PCL as the shell material, the PDI seemed not to be affected by the TLC as the *P*-values obtained were higher than 0.05 ($P = 0.06$ in the case of tyrosol-loaded PLGA microparticles and $P = 0.84$ in the case of tyrosol-loaded PCL microparticles).

In the case of tyrosol-loaded EC microparticles, an increase of the TLC led to an increase of the polydispersity. This observation is also in agreement with the conclusions drawn when hydroxytyrosol was encapsulated in EC microparticles: the PDI increased from 2.9 ± 0.1 to 5.5 ± 0.3 when the theoretical loading content was shifted from 5 to 10% *w/w* (Paulo and Santos 2018b).

However, it should be considered that a considerable number of factors (e.g., formulation and process factors) may affect the mean particle size, particle size distribution as well as the polydispersity of microparticles (Krishnamachari et al. 2007; Paulo and Santos 2018b).

The obtained results regarding the evaluation of the particle size distribution are significative. The mean particle size of both tyrosol-loaded PLGA and EC microparticles was dependent on the TLC: an increase of the loading content led to an increase of the mean particle size. Dissimilarly, the mean particle size of tyrosol-loaded PCL microparticles was not affected by the TLC. Moreover, in the case of using PLGA and EC as coating materials, microparticles formulated with a TLC of 5% *w/w* present a unimodal particle size distribution whereas microparticles formulated with TLC of 10% *w/w* present a multimodal particle size distribution.

Considering the polydispersity of the obtained microparticles, it can be stated that only for tyrosol-loaded EC microparticles, the PDI was dependent on the loading content. In this case, an increase in the loading content led to an increase in the PDI of the obtained powder.

Evaluation of the Total Antioxidant Capacity

The Cu^{2+} chelating activity was evaluated for free tyrosol (tyrosol aqueous solutions with a concentration corresponding to the TLC chosen for the present study) and encapsulated tyrosol using three alternative polymer-carriers. The main goal was to evaluate the free radical scavenging capacity of tyrosol and tyrosol-loaded microparticles.

Alternative methodologies can be employed to quantify the radical scavenging capacity of pure compounds and the corresponding microparticles as the (i) the application of the 2,2-diphenyl-1-picrylhydrazyl (DPPH) radical scavenging methodology, (ii) the use of the 2,2′-azinobis(3-ethylbenzothiazoline-6-sulfonic acid) diammonium salt (ABTS) radical scavenging methodology, (iii) using the oxygen radical absorbance capacity (ORAC) assay, (iv)

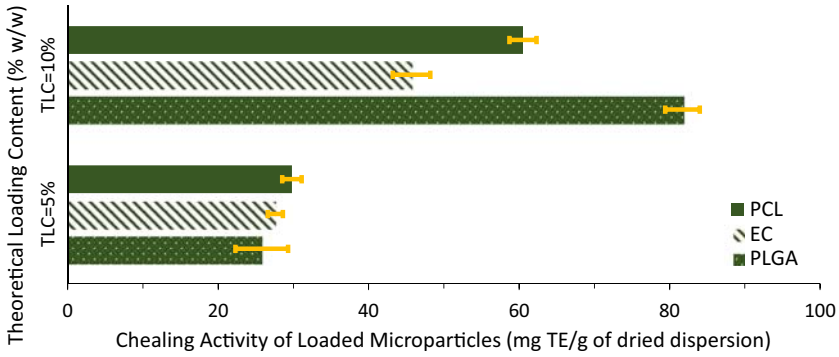

Fig. 9 Cu^{2+} chelating activity of tyrosol-loaded microparticles (mg TE/g of tyrosol) (EC, ethycellulose; PCL, polycaprolactone; PLGA, poly(D,L-lactide-*co*-glycolide; TE, Trolox equivalents; TLC, theoretical loading content). Data are expressed as mean ± standard deviation of three independent assays. The yellow bars correspond to the error bars based on the standard deviation of three independent assays

applying the superoxide dismutase (SOD) assay, or even (v) using the ferric reducing antioxidant potential (FRAP) assay, among others (Dudonné et al. 2009).

The authors Jabeen et al. (2017) reported the application of Cu^{2+}-antioxidant complex formation for the radical scavenging determination. In the present study, this alternative method was employed in order to assess the radical scavenging capacity of tyrosol and tyrosol-loaded microparticles.

The total antioxidant capacity of tyrosol-loaded microparticles (expressed as mg of TE/g of tyrosol) versus the theoretical loading content (% *w/w*) is presented in Fig. 9.

For the TLC of 5% *w/w*, the working solution presented a total antioxidant capacity of 106 ± 4 mg of TE/L (0.4 ± 0.1 mM of TE) and the working solution used for the encapsulation of tyrosol considering a TLC of 10% *w/w* showed an antioxidant capacity of 126 ± 18 mg of TE/L (0.5 ± 0.1 mM of TE). It was verified that the Cu^{2+} chelating activity of tyrosol was not proportional to the amount of tyrosol dissolved in ultrapure water—the amount of tyrosol dissolved in ultrapure water was doubled from the working solution used for the obtainment of tyrosol-loaded microparticles with a TLC of 5 to 10% *w/w*; however, the Cu^{2+} chelating activity of tyrosol only increased 18.3% from the theoretical loading content of 5 to 10% *w/w*.

In the case of tyrosol-loaded PLGA microparticles formulated considering a TLC of 5% *w/w* and 10% *w/w*, the mean antioxidant capacity (Cu^{2+} chelating capacity) was 26 ± 4 mg of TE/g of dried dispersion and 82 ± 2 mg of TE/g of dried dispersion, respectively.

Regarding the results of the Cu^{2+} chelating capacity of tyrosol-loaded EC microparticles, the mean antioxidant capacity encapsulated was 28 ± 1 mg of TE/g of dried dispersion in the case of TLC of 5% *w/w* and 46 ± 3 mg of TE/g of dried powder when considered the TLC of 10% *w/w*.

When PCL was used as the polymer-carrier of tyrosol, the Cu^{2+} chelating capacity of loaded microparticles was 30 ± 1 mg of TE/g of dried microparticles in the case of the TLC of 5% *w/w* and 61 ± 2 mg of TE/g of microparticles (dry basis) when the TLC of 10% *w/w* was considered.

Regarding the statistical analysis, it can be stated that, when the results are grouped by TLC, for all the polymer-carriers studied, the TLC seemed to affect the Cu^{2+} chelating capacity of loaded microparticles as the *P* values were found to be lower than 0.05 for all the polymers ($P = 2.00 \times 10^{-5}$ in the case of tyrosol-loaded PLGA microparticles, $P = 2.70 \times 10^{-4}$ respecting to tyrosol-loaded EC microparticles and $P = 4.61 \times 10^{-5}$ in the case of loaded microparticles formulated with PCL). When the results were grouped by the polymer, for the two TLC studied, it was verified that in the case of a TLC of 5% *w/w*, the polymer chosen did not affect the Cu^{2+} chelating capacity of loaded microparticles ($P = 0.19 > 0.05$). In the case of microparticles formulated considering a TLC of 10% *w/w*, the Cu^{2+} chelating capacity of loaded microparticles was significantly affected by the polymer chosen ($P = 4.40 \times 10^{-6} < 0.05$).

The presented results are significant as not only they prove that tyrosol was efficiently incorporated in distinctive polymer-carriers as it shows that the mean antioxidant capacity encapsulated was dependent of the theoretical loading content for the polymers studied, independent of the polymer chosen when selected powders formulated with a TLC of 5% *w/w* and dependent of the polymer-carrier in the case of considering a TLC of 10% *w/w*.

These results bring new insights for the encapsulation of antioxidants in polymer matrices intended for food, pharmaceutical, cosmetic, and nutraceutical applications—in the specific case of the powerful antioxidant tyrosol, the antioxidant capacity of loaded microparticles can be tailored-made for the matrices reported.

Conclusions

The worldwide recognition of the health benefits of the Mediterranean dietary pattern has fostered the consumption of olive oil as the preferential fat source. Tyrosol is a powerful antioxidant present in high quantitates in olive oil and olive mill wastes. Even though it presents beneficial properties, its incorporation as a free compound in foods and other matrices

is still limited. Therefore, water-in-oil-in-water double emulsion solvent evaporation technique may be applied to encapsulate this compound for further incorporation in foods and other alternative matrices.

The results of this study demonstrate that the Fourier transform infrared spectroscopy confirmed the efficient incorporation of tyrosol in the polymer matrices selected for this study. Tyrosol-loaded microparticles were thermogravimetrically stable in the temperature range of 30 to 261 °C, and polycaprolactone was considered to be an exceptional carrier regarding the thermogravimetric stability of microparticles. It was observed that an increase in the theoretical loading content led to an increase in the agglomeration degree of microparticles.

The production yield was dependent on the loading content for both poly(D,L-lactide-*co*-glycolide) and ethylcellulose. The encapsulation efficiency was dependent on the loading content in the case of using polycaprolactone as a coating material. In the case of using poly(D,L-lactide-*co*-glycolide) and ethylcellulose as polymer-carriers of tyrosol, it was verified that an increase of the theoretical loading content from 5 to 10% *w/w* led to a decrease of production yield. It was also verified that an increase of the loading content led to a decrease in the production yield when polycaprolactone was used as a polymer-carrier for tyrosol.

The results of this study on the encapsulation of tyrosol using alternative polymer-carriers bring new insights regarding the encapsulation of natural antioxidants and antioxidant-rich extracts obtained from olives, olive oil, and olive mill wastes intended for further incorporation in food, pharmaceutical, cosmetic, and nutraceutical matrices.

Funding information This work was financially supported by project UID/EQU/00511/2019 - Laboratory for Process Engineering, Environment, Biotechnology, and Energy – LEPABE funded by national funds through FCT/MCTES (PIDDAC). This work was developed under the doctoral program in Chemical and Biological Engineering (PDEQB), financially supported by the grant NORTE-08-5369-FSE-000028, co-financed by the Northern Regional Operational Program (NORTE 2020) through Portugal 2020 and the European Social Fund (ESF).

Compliance with Ethical Standards

Conflict of Interest The authors declare that they have no conflict of interest.

References

Aguiar, J., Estevinho, B. N., & Santos, L. (2016). Microencapsulation of natural antioxidants for food application – The specific case of coffee antioxidants – A review. *Trends in Food Science and Technology, 58*, 21–39. https://doi.org/10.1016/j.tifs.2016.10.012.

Aguiar, J., Costa, R., Rocha, F., Estevinho, B. N., & Santos, L. (2017). Design of microparticles containing natural antioxidants: Preparation, characterization and controlled release studies. *Powder Technology, 313*, 287–292. https://doi.org/10.1016/j.powtec.2017.03.013.

Aldini, G., Piccoli, A., Beretta, G., Morazzoni, P., Riva, A., Marinello, C., & Maffei Facino, R. (2006). Antioxidant activity of polyphenols from solid olive residues of c.v. Coratina. *Fitoterapia, 77*(2), 121–128. https://doi.org/10.1016/j.fitote.2005.11.010.

Benavente-García, O., Castillo, J., Lorente, J., Ortuño, A., & Del Rio, J. A. (2000). Antioxidant activity of phenolics extracted from Olea europaea L. leaves. *Food Chemistry, 68*(4), 457–462. https://doi.org/10.1016/S0308-8146(99)00221-6.

Benbettaïeb, N., Karbowiak, T., Brachais, C.-H. & Debeaufort, F. (2015). Coupling tyrosol, quercetin or ferulic acid and electron beam irradiation to cross-link chitosan–gelatin films: A structure – function approach. *European Polymer Journal, 67*, 113–127. https://doi.org/10.1016/j.eurpolymj.2015.03.060.

Carluccio, M. A., Siculella, L., Ancora, M. A., Massaro, M., Scoditti, E., Storelli, C., & Caterina, R. D. (2003). Olive oil and red wine antioxidant polyphenols inhibit antiatherogenic properties of Mediterranean diet phytochemicals. *Arteriosclerosis, Thrombosis, and Vascular Biology, 23*, 622–629. https://doi.org/10.1161/01.ATV.0000062884.69432.A0.

Castro-quezada, I., Román-viñas, B., & Serra-majem, L. (2014). The Mediterranean diet and nutritional adequacy: A review. *Nutrients, 6*, 231–248. https://doi.org/10.3390/nu6010231.

Chandramohan, R., Pari, L., Rathinam, A., & Sheikh, B. A. (2015). Chemico-Biological Interactions Tyrosol , a phenolic compound , ameliorates hyperglycemia by regulating key enzymes of carbohydrate metabolism in streptozotocin induced diabetic rats. *Chemico-Biological Interactions, 229*, 44–54. https://doi.org/10.1016/j.cbi.2015.01.026.

Chang, C. Y., Huang, I. T., Shih, H. J., Chang, Y. Y., Kao, M. C., Shih, P. C., & Huang, C. J. (2019). Cluster of differentiation 14 and toll-like receptor 4 are involved in the anti-inflammatory effects of tyrosol. *Journal of Functional Foods, 53*, 93–104. https://doi.org/10.1016/j.jff.2018.12.011.

Chen, D. R., Bei, J. Z., & Wang, S. G. (2000). Polycaprolactone microparticles and their biodegradation. *Polymer Degradation and Stability, 67*, 455–459. https://doi.org/10.1016/S0141-3910(99)00145-7.

Cicerale, S., Lucas, L. J., & Keast, R. S. J. (2012). Antimicrobial, antioxidant and anti-inflammatory phenolic activities in extra virgin olive oil. *Current Opinion in Biotechnology, 23*(2), 129–135. https://doi.org/10.1016/j.copbio.2011.09.006.

Couto, E., Boffetta, P., Lagiou, P., Ferrari, P., Buckland, G., Overvad, K., & Sa, M. (2011). Mediterranean dietary pattern and cancer risk in the EPIC cohort. *British Journal of Cancer, 104*, 1493. https://doi.org/10.1038/bjc.2011.106.

Danhier, F., Ansorena, E., Silva, J. M., Coco, R., Le, A., & Préat, V. (2012). PLGA-based nanoparticles: An overview of biomedical applications. *Journal of Controlled Release, 161*(2), 505–522. https://doi.org/10.1016/j.jconrel.2012.01.043.

Dasaratha, M., & Sathyamoorthy, N. (2018). Preparation of poly (epsilon-caprolactone) microspheres containing etoposide by solvent evaporation method. *Asian Journal of Pharmaceutical Sciences, 5*, 114–122.

De Marco, E., Savarese, M., Paduano, A., & Sacchi, R. (2007). Characterization and fractionation of phenolic compounds extracted from olive oil mill wastewaters. *Food Chemistry, 104*(2), 858–867. https://doi.org/10.1016/j.foodchem.2006.10.005.

Dubernet, C. (1995). Thermoanalysis of microspheres. *Thermochimica Acta, 248*, 259–269. https://doi.org/10.1016/0040-6031(94)01947-F.

Dudonné, S., Vitract, X. C., Woillez, P., & Marion Mérillon, J.-M. (2009). Comparative study of antioxidant properties and total phenolic content of 30 plant extracts of industrial interest using DPPH, ABTS, FRAP, SOD, and ORAC assays. *Journal of Agricultural and Food Chemistry, 57*, 1768–1774.

El, S. N., & Karakaya, S. (2009). Olive tree (Olea europaea) leaves: Potential beneficial effects on human health. *Nutrition Reviews, 67*(11), 632–638. https://doi.org/10.1111/j.1753-4887.2009.00248.x.

El-Abbassi, A., Kiai, H., & Hafidi, A. (2012). Phenolic profile and antioxidant activities of olive mill wastewater. *Food Chemistry, 132*(1), 406–412. https://doi.org/10.1016/j.foodchem.2011.11.013.

Fernández-mar, M. I., Mateos, R., García-parrilla, M. C., Puertas, B., & Cantos-villar, E. (2012). Bioactive compounds in wine: Resveratrol , hydroxytyrosol and melatonin: A review. *Food Chemistry, 130*, 797–813. https://doi.org/10.1016/j.foodchem.2011.08.023.

Freytag, T., Dashevsky, A., Tillman, L., Hardee, G. E., & Bodmeier, R. (2000). Improvement of the encapsulation efficiency of oligonucleotide-containing biodegradable microspheres. *Journal of Controlled Release, 69*(1), 197–207. https://doi.org/10.1016/S0168-3659(00)00299-6.

Friess, W., & Schlapp, M. (2002). Release mechanisms from gentamicin loaded poly(lactic-co-glycolic acid) (PLGA) microparticles. *Journal of Pharmaceutical Sciences, 91*(3), 845–855. https://doi.org/10.1002/jps.10012.

Gabor, F., Ertl, B., Wirth, M., & Mallinger, R. (1999). Ketoprofen-poly(D,L-lactide-co-glycolic acid) microspheres: influence of manufacturing parameters and type of polymer on the release characteristics. *Journal of Microencapsulation, 16*(1), 1–12.

Giovannini, C., Straface, E., Modesti, D., Coni, E., Cantafora, A., De Vincenzi, M., & Masella, R. (1999). Tyrosol, the major olive oil biophenol, protects against oxidized-LDL-induced injury in Caco-2 cells. *Journal of Nutrition, 129*(7), 1269–1277. https://doi.org/10.1093/jn/129.7.1269.

Gómez-gracia, E., Ruiz-gutiérrez, V., & Fiol, M. (2018). Primary prevention of cardiovascular disease with a Mediterranean diet. *New England Journal, 378*(25), 1279–1290. https://doi.org/10.1056/NEJMoa1200303.

Hill, L. E., Gomes, C., & Taylor, T. M. (2013). Characterization of beta-cyclodextrin inclusion complexes containing essential oils (trans-cinnamaldehyde, eugenol, cinnamon bark, and clove bud extracts) for antimicrobial delivery applications. *LWT - Food Science and Technology, 51*(1), 86–93. https://doi.org/10.1016/j.lwt.2012.11.011.

Ibraheem, D., Iqbal, M., Agusti, G., Fessi, H., & Elaissari, A. (2014). Effects of process parameters on the colloidal properties of polycaprolactone microparticles prepared by double emulsion like process. *Colloids and Surfaces A: Physicochemical and Engineering Aspects, 445*, 79–91. https://doi.org/10.1016/j.colsurfa.2014.01.012.

Jabeen, E., Kausar, N., Ahmed, S., Murtaza, I., Ali, T., & Hameed, S. (2017). Radical scavenging propensity of Cu^{2+}, Fe^{3+} complexes of fl avonoids and in-vivo radical scavenging by Fe^{3+} −primuletin. *Spectrochimica Acta Part A: Molecular and Biomolecular Spectroscopy, 171*, 432–438. https://doi.org/10.1016/j.saa.2016.08.035.

Jansen-Alves, C., Maia, D. S. V., Krumreich, F. D., Crizel-cardoso, M. M., Fioravante, J. B., Wladimir, P., & Zambiazi, R. C. (2019). Propolis microparticles produced with pea protein : Characterization and evaluation of antioxidant and antimicrobial activities. *Food Hydrocolloids, 87*, 703–711. https://doi.org/10.1016/j.foodhyd.2018.09.004.

Jyothi, N. V. N., Prasanna, P. M., Sakarkar, S. N., Prabha, K. S., Ramaiah, P. S., & Srawan, G. Y. (2010). Microencapsulation techniques, factors influencing encapsulation efficiency. *Journal of Microencapsulation, 27*(3), 187–197. https://doi.org/10.3109/02652040903131301.

Karathanos, V. T., Mourtzinos, I., Yannakopoulou, K., & Andrikopoulos, N. K. (2007). Study of the solubility, antioxidant activity and structure of inclusion complex of vanillin with β-cyclodextrin. *Food Chemistry, 101*(2), 652–658. https://doi.org/10.1016/j.foodchem.2006.01.053.

Krishnamachari, Y., Madan, P., & Lin, S. (2007). Development of pH- and time-dependent oral microparticles to optimize budesonide delivery to ileum and colon. *International Journal of Pharmaceutics, 338*(1–2), 238–247. https://doi.org/10.1016/j.ijpharm.2007.02.015.

Labet, M., & Thielemans, W. (2009). Synthesis of polycaprolactone: A review. *Chemical Society Reviews, 38*(12), 3484–3504. https://doi.org/10.1039/b820162p.

Lee, H., Won, S., Hwa, C., Jin, Y., & Youl, T. (2016). Tyrosol, an olive oil polyphenol, inhibits ER stress-induced apoptosis in pancreatic b-cell through JNK signaling. *Biochemical and Biophysical Research Communications, 469*(3), 748–752. https://doi.org/10.1016/j.bbrc.2015.12.036.

Lesage-Meessen, L., Navarro, D., Maunier, S., Sigoillot, J. C., Lorquin, J., Delattre, M., & Labat, M. (2001). Simple phenolic content in olive oil residues as a function of extraction systems. *Food Chemistry, 75*(4), 501–507. https://doi.org/10.1016/S0308-8146(01)00227-8.

Ling, M., Chih, Y., Jaw, G., Ting, H., Ken, J., Hsien, T., & Kuang, C. (2008). Controlled release carrier of BSA made by W / O / W emulsion mmethod containing PLGA and hydroxyapatite. *Journal of Controlled Release, 128*, 142–148. https://doi.org/10.1016/j.jconrel.2008.02.012.

Makadia, H., & Siegel, S. (2012). Poly lactic-co-glycolic acid (PLGA) as biodegradable controlled drug delivery carrier. *Polymers, 3*(3), 1–19. https://doi.org/10.3390/polym3031377.

Malheiro, R., Casal, S., Sousa, A., & Pinho, P. G. De. (2012). Effect of cultivar on sensory characteristics, chemical composition, and nutritional value of stoned green table olives. *Food and Bioprocess Technology, 5*, 1733–1742. https://doi.org/10.1007/s11947-011-0567-x.

Mandal, T. K., Bostanian, L. A., Graves, R. A., & Chapman, S. R. (2002). Encapsulated poly (vinyl alcohol) hydrogel as a drug delivery system. *Pharmaceutial Research, 19*(11), 1713–1718.

Mitrou, P. N., Kipnis, V., Thie, A. C. M., Subar, A. F., & Wirfa, E. (2015). Mediterranean dietary pattern and prediction of all-cause mortality in a US population. *JAMA Internal Medicine, 167*(22), 2461–2468. https://doi.org/10.1001/archinte.167.22.2461.

Murtaza, G. (2012). Ethylcellulose microparticles: a review. *Acta Poloniae Pharmaceutica Drug Research, 69*(1), 11–22.

Nadtochiy, S. M., Ph, D., & Redman, E. K. (2011). Mediterranean diet and cardioprotection: The role of nitrite, polyunsaturated fatty acids, and polyphenols. *Nutrition, 27*(7–8), 733–744. https://doi.org/10.1016/j.nut.2010.12.006.

Nagy, J. B., David, C., De Kesel, C., & Lefe, C. (1999). Blends of polycaprolactone with polyvinylalcohol: a DSC, optical microscopy and solid state NMR study. *Polymer, 40*, 1969–1978. https://doi.org/10.1016/S0032-3861(98)00253-5.

Natarajan, V., Krithica, N., Madhan, B., & Sehgal, P. K. (2011). Formulation and evaluation of quercetin polycaprolactone microspheres for the treatment of rheumatoid arthritis. *Journal of Pharmaceutical Sciences, 100*(1), 195–205. https://doi.org/10.1002/jps.22266.

Obied, H. K., Bedgood, D. R., Prenzler, P. D., & Robards, K. (2007). Bioscreening of Australian olive mill waste extracts: Biophenol content, antioxidant, antimicrobial and molluscicidal activities. *Food and Chemical Toxicology, 45*(7), 1238–1248. https://doi.org/10.1016/j.fct.2007.01.004.

Pamujula, S., Graves, R. A., Freeman, T., Srinivasan, V., Bostanian, L. A., Kishore, V., & Mandal, T. K. (2004). Oral delivery of spray dried PLGA/amifostine nanoparticles. *The Journal of Pharmacy and Pharmacology, 56*(9), 1119–1125. https://doi.org/10.1211/0022357044210.

Pamujula, S., Graves, R. A., Moiseyev, R., Bostanian, L. A., Kishore, V., & Mandal, T. K. (2008). Preparation of polylactide-co-glycolide and chitosan hybrid microcapsules of amifostine using coaxial ultrasonic atomizer with solvent evaporation. *Journal of Pharmacy and*

Pharmacology, 60(3), 283–289. https://doi.org/10.1211/jpp.60.3.0002.

Paulo, F., & Santos, L. (2018a). Double emulsion solvent evaporation approach as a novel eugenol delivery system – Optimization by response surface methodology. *Industrial Crops and Products, 126*, 287–301. https://doi.org/10.1016/j.indcrop.2018.10.027.

Paulo, F., & Santos, L. (2018b). Inclusion of hydroxytyrosol in ethyl cellulose microparticles: In vitro release studies under digestion conditions. *Food Hydrocolloids, 84*, 104–116. https://doi.org/10.1016/j.foodhyd.2018.06.009.

Paulo, F., & Santos, L. (2019). Microencapsulation of caffeic acid and its release using a w/o/w double emulsion method: Assessment of formulation parameters. *Drying Technology, 37*, 950–961. https://doi.org/10.1080/07373937.2018.1480493.

Pereira, A. P., Ferreira, I. C. F. R., Marcelino, F., Valentão, P., Andrade, P. B., Seabra, R., & Pereira, J. A. (2007). Phenolic compounds and antimicrobial activity of olive (Olea europaea L. Cv. Cobrançosa) leaves. *Molecules, 12*(5), 1153–1162. https://doi.org/10.3390/12051153.

Petroni, A., Salami, M., Papini, N., Montedorol, G. F., & Galli, C. (1995). Inhibition of platelet aggregation and eicosanoid production by phenolic components of olive oil. *Thrombosis Research, 78*(2), 151–160. https://doi.org/10.1016/0049-3848(95)00043-7.

Piletti, R., Bugiereck, A. M., Pereira, A. T., Gussati, E., Dal Magro, J., Mello, J. M. M., & Fiori, M. A. (2017). Microencapsulation of eugenol molecules by β-cyclodextrine as a thermal protection method of antibacterial action. *Materials Science and Engineering C, 75*, 259–271. https://doi.org/10.1016/j.msec.2017.02.075.

Preedy, V. R., & Watson, R. R. (2017). *Olives and olive oil in health and disease prevention* (Vol. 91, pp. 1225–1232). Elsevier.

Ruiz-gutie, V., Romaguera, D., & Marti, M. A. (2017). Prediction of cardiovascular disease by the Framingham-REGICOR equation in the high-risk PREDIMED cohort: Impact of the Mediterranean diet across different risk strata. *Journal of the American Heart Association*, 6. https://doi.org/10.1161/JAHA.116.004803.

Salucci, S., Burattini, S., Battistelli, M., Buontempo, F., Canonico, B., Maria, A., & Falcieri, E. (2015). Tyrosol prevents apoptosis in irradiated keratinocytes. *Journal of Dermatological Science, 80*(1), 61–68. https://doi.org/10.1016/j.jdermsci.2015.07.002.

Sato, K., Mihara, Y., Kanai, K., Yamashita, Y., Kimura, Y., Itoh, N., et al. (2016). Tyrosol ameliorates lipopolysaccharide-induced ocular inflammation in rats via inhibition of nuclear factor (NF)-kappaB activation. *The Journal of Veterinary Medical Science, 78*(9), 1429–1438. https://doi.org/10.1292/jvms.16-0166.

Serra, G., Deiana, M., Spencer, J. P. E., & Corona, G. (2017). Olive oil phenolics prevent oxysterol-induced proinflammatory cytokine secretion and reactive oxygen species production in human peripheral blood mononuclear cells, through modulation of p38 and JNK pathways. *Molecular Nutrition and Food Research, 61*(12), 1–27. https://doi.org/10.1002/mnfr.201700283.

Sofi, F., Abbate, R., Gensini, G. F., & Casini, A. (2010). Accruing evidence on benefits of adherence to the Mediterranean diet on health: An updated systematic review and meta-analysis. *The American Journal of Clinical Nutrition, 92*(5), 1189–1196. https://doi.org/10.3945/ajcn.2010.29673.

Sofi, F., Macchi, C., Abbate, R., Gensini, G. F., & Casini, A. (2013). Mediterranean diet and health. *Biofactors, 39*(4), 335–342. https://doi.org/10.1002/biof.1096.

Tasioula-Margari, M., & Tsabolatidou, E. (2015). Extraction, separation, and identification of phenolic compounds in virgin olive oil by HPLC-DAD and HPLC-MS. *Antioxidants, 4*(3), 548–562. https://doi.org/10.3390/antiox4030548.

Troya, D., Tupuna-Yerovi, D., & Ruales, J. (2018). Effects of wall materials and operating parameters on physicochemical properties, process efficiency, and total carotenoid content of microencapsulated banana passionfruit pulp (Passiflora tripartita var. mollissima) by spray-drying. *Food and Bioprocess Technology, 11*, 1828–1839. https://doi.org/10.1007/s11947-018-2143-0.

Tuck, K. L., & Hayball, P. J. (2002). Major phenolic compounds in olive oil: Metabolism and health effects. *Journal of Nutritional Biochemistry, 13*(11), 636–644. https://doi.org/10.1016/S0955-2863(02)00229-2.

UNESCO. (2013). Mediterranean diet. Retrieved January 22, 2019, from https://ich.unesco.org/en/RL/mediterranean-diet-00884.

Veiga, F., & Cla, A. (2011). New delivery systems to improve the bioavailability of resveratrol. *Expert Opinion on Drug Delivery, 8*, 973–990. https://doi.org/10.1517/17425247.2011.581655.

Visioli, F., Romani, A., Mulinacci, N., Zarini, S., Conte, D., Vincieri, F. F., & Galli, C. (1999). Antioxidant and other biological activities of olive mill waste waters. *Journal of Agricultural and Food Chemistry, 47*(8), 3397–3401. https://doi.org/10.1021/jf9900534.

Vlachogianni, I. C., Fragopoulou, E., Kostakis, I. K., & Antonopoulou, S. (2015). In vitro assessment of antioxidant activity of tyrosol, resveratrol and their acetylated derivatives. *Food Chemistry, 177*, 165–173. https://doi.org/10.1016/j.foodchem.2014.12.092.

Yekdane, N., & Goli, S. (2019). Effect of pomegranate juice on characteristics and oxidative stability of microencapsulated pomegranate seed oil using spray drying. *Food and Bioprocess Technology, 12*, 1614–1625. https://doi.org/10.1007/s11947-019-02325-8.

Yoksan, R., Jirawutthiwongchai, J., & Arpo, K. (2010). Encapsulation of ascorbyl palmitate in chitosan nanoparticles by oil-in-water emulsion and ionic gelation processes. *Colloids and Surfaces B: Biointerfaces, 76*(1), 292–297. https://doi.org/10.1016/j.colsurfb.2009.11.007.

Zhang, H., & Gao, S. (2007). Temozolomide/PLGA microparticles and antitumor activity against Glioma C6 cancer cells *in vitro*. *International Journal of Pharmaceuticals, 329*, 122–128. https://doi.org/10.1016/j.ijpharm.2006.08.027.

Zhou, D., Sun, Y., & Shahidi, F. (2017). Preparation and antioxidant activity of tyrosol and hydroxytyrosol esters. *Journal of Functional Foods, 37*, 66–73. https://doi.org/10.1016/j.jff.2017.06.042.